AN EXPERIMENTAL INVESTIGATION OF THE STABILITY OF THE HYPERSONIC LAMINAR BOUNDARY LAYER

Thesis by

Anthony Demetriades

In Partial Fulfillment of the Requirements

For the Degree of

Doctor of Philosophy

California Institute of Technology

Pasadena, California

1958

ACKNOWLEDGMENTS

The research described herein was carried out under the supervision of Professor Lester Lees whose guidance and helpfulness merit the author's utmost gratitude. The author also acknowledges with much appreciation the help of Dr. John Laufer of the Jet Propulsion Laboratory who very kindly and patiently offered the author invaluable suggestions. Thanks are due to Mr. William Sublette for fabricating the experimental models and to Mrs. N. Kindig and Mrs. B. Wood for helping in preparing the figures; special thanks are also due to Mrs. Geraldine Van Gieson for typing the manuscript with her usual care and dexterity.

ABSTRACT

An experimental investigation of the stability of the hypersonic laminar boundary layer was carried out for the case of a flat insulated surface at zero angle of attack. The stream-wise amplitude variation of both "natural" disturbances (i. e., flow fluctuations existing naturally in the boundary layer) and of disturbances artificially excited with a "siren" mechanism was studied with the aid of a hot-wire anemometer. In both cases it was found that such small fluctuations amplify for certain ranges of the fluctuation frequency and the Reynolds number R_θ, and damp for others. The demarcation boundaries for the amplification (instability) zone were found to resemble the corresponding boundaries of boundary layer instability at lower speeds. A "line of maximum amplification" of disturbances was also found. The amplification rates and hence the degree of "selectivity" of the hypersonic layer were found, however, to be considerably lower than those at the lower speeds. The disturbances selected by the layer for maximum amplification have a wavelength estimated at about twenty times the boundary-layer thickness δ, which is appreciably longer than the corresponding wave-lengths for low-speed boundary-layer flow.

TABLE OF CONTENTS

PART		PAGE
	Acknowledgments	ii
	Abstract	iii
	Table of Contents	iv
	List of Tables	vi
	List of Figures	vii
	List of Symbols	x
I.	Introduction	1
II.	Definition of the Problem	5
III.	The Experimental Method	10
IV.	Facilities and Equipment	14
	A. Wind Tunnel	14
	B. Flat Plate Models	14
	1. Survey Plate	14
	2. Siren Plate	14
	C. Hot-Wire Anemometer Probe	16
	D. Electronic Instrumentation	17
	E. Hot-Wire Technique	18
V.	The Flow Field	20
	A. Boundary Layer Flow over the Flat Plate Models	20
	B. Free Stream Turbulence	23

VI. Measurements of the Natural Fluctuations 27

A. Measurements at Constant Frequency 27

B. The Line of Maximum Amplification 28

C. Summary 31

VII. Measurement of the Artificial Fluctuations 32

VIII. The Critical Layer 38

IX. Suggested Extensions of the Work 41

X. Conclusions 42

References 43

Tables 46

Figures 51

LIST OF TABLES

NUMBER	TITLE	PAGE
1	Typical Operating Conditions for the Hot-Wire Anemometer	46
2	Extrema in the Amplitude Variation of the Natural Fluctuations (Survey Plate)	47
3	Maximum-Amplification-Line Data (Natural Fluctuations)	48
4	Extrema in the Amplitude Variation of the Artificial Fluctuations (Siren Plate)	49

LIST OF FIGURES

NUMBER	TITLE	PAGE
1	Schematic Presentation of the Stable and Unstable Regions for a Laminar Boundary Layer	51
2	Schematic Diagram of GALCIT Leg 1 Hypersonic Tunnel Test Section Showing Flat Plate and Probe Installation	52
3	Schematic Drawing of Flat Plate Model with "Siren" Mechanism	53
4	Photograph of the Siren Plate (Right) with the Cover Plate (Left)Removed	54
5	Hot-Wire Anemometer Probe as Installed in Leg 1 of the Hypersonic Tunnel	55
6	Exploded Schematic View of the Hot-Wire Anemometer Probe Head	56
7	Microcomparator Photograph of a 0.0001"-Diameter Hot-Wire Mounted on the Probe Needle Tips	57
8	Photograph of the Test Section of the GALCIT Leg 1 Hypersonic Tunnel Showing: A. Probe Sleeve Supports; B. Probe Strut; C. Flat Plate Support; D. Flat Plate Model	58
9	Wheatstone Bridge, Heating Circuit and Scheme of Compensation for Hot-Wire R_w Thermal Lag	59
10(a)	Block Diagram of Electronic Instrumentation for Hot-Wire Measurements	60
10(b)	Frequency Response Curve of the Preamplifier	61
10(c)	Frequency Response Curve of the Compensating Amplifier	61
10(d)	Typical Overall Frequency Response of the System Wire-Preamplifier-Compensating Amplifier	61
10(e)	Response of the Band-Pass Filter Rejecting All Frequencies Above and Below n	61

11	Boundary Layer Growth on Survey Plate (Solid Lines) and Siren Plate (Points) Along Centerline	62
12	Momentum Thickness Growth on Survey Plate (Solid Lines) and Siren Plate (Points) Along Centerline	62
13	Variation of Reynolds No. R_θ for a Flat Plate at Zero Incidence at M = 5.8, T_o = 225°F Based on Figures 11 and 12	63
14	Similarity of Boundary Layer Profiles Along the Centerline of the Survey Plate	64
15	Variation of Plate Surface Pressure P/P_o Distribution with Distance y of Hot-Wire Probe Above Surface	65
16	Variation of Fluctuation Energy Spectrum with Position Along Tunnel Centerline. P_o = 50 psig.	66
17	Variation of Hot-Wire Sensitivity Coefficients in Hypersonic Flow. M = 5.8, T_o = 225°F	67
18	Variation of the Parameter $2\pi \nu_\infty / U_\infty^2$ with Supply Pressure for M = 5.8 and T_o = 225°F	68
19	Typical Hot-Wire Output Intensity Variations Due to Natural Fluctuations	69
20	Typical Variation of Hot-Wire Output Intensity Due to Natural Fluctuations	70
21	The Locus of Maxima (Upper Neutral Branch) in the Amplitude Variation of Natural Fluctuations. Numbers Identify Data Points of Table 2	71
22	Hot-Wire Mean-Square Output Spectra in the Laminar Boundary Layer. M = 5.8, T_o = 225°F	72
23	Points Defining the "Line of Maximum Amplification"	73
24	Typical Variation of Hot-Wire Mean-Square Output Spectrum Across Layer at $R_\theta \simeq 1400$	74
25	Typical Response of the Hot-Wire at Location (x, y) to Air Injection Through the Siren Slit	75

26	Aspect of the Fluctuations Induced into the Laminar Hypersonic Boundary Layer with the Siren Mechanism	76
27	Variation in the Amplitude of the Artificial Fluctuations with Position of x of the Wire in the Boundary Layer as Viewed with the Display-Type Wave Analyzer	77
28	Typical Hot-Wire Output Variations Due to Artificial Fluctuations	78
29	Typical Hot-Wire Output Variations Due to Artificial Fluctuations	79
30	Typical Hot-Wire Output Variations Due to Artificial Fluctuations	80
31	Upper and Lower Neutral Stability Branches for Artificial Fluctuations	81
32	Experimentally Determined Boundary Layer Stability for Various Mach Numbers	82
33	Comparison of Signal Level and Distribution with and without the Siren and without the Flat Plate	83
34	Variation Across the Laminar Boundary Layer of the Hot-Wire Output Integrated over All Frequencies	84
35	Wave Number a_θ vs. R_θ for Neutral Stability of the Boundary Layer	85

LIST OF SYMBOLS

A	$= q(y)\, e^{a c_i t}$ = total fluctuation amplitude
A_w'	hot-wire overheating parameter $= \frac{i}{2} \frac{1}{R_w} \left(\frac{\partial R_w}{\partial i} \right)$
c	fluctuation velocity $= c_r + i\, c_i$
c_G	fluctuation group velocity
c_r	fluctuation phase velocity
e_m	coefficient of hot-wire sensitivity to changes in the fluid mass flow
e_T	coefficient of hot-wire sensitivity to changes in the fluid total temperature
f	fluctuation frequency
F	Froude number
i	current through hot-wire; also, current through output thermocouple
$\dot{m}$	rate of mass-injection through siren slits
M	Mach number
M'	time constant of hot-wire
P	pressure
q	fluctuation amplitude distribution across boundary layer
Q'	time-dependent flow fluctuation
R_{m_T}	correlation coefficient between mass-flow and total temperature fluctuations
R_w	hot-wire resistance
R_θ	Reynolds number based on momentum thickness $= \frac{\rho_\infty U_\infty \theta}{\mu_\infty}$
t	time
T	temperature

U, u	velocity in x- direction
w	electrical power dissipated by the hot-wire anemometer
x	streamwise coordinate
y	coordinate in direction normal to solid surface
a	$2\pi/\lambda$ (wave number)
a_θ	$2\pi\theta/\lambda$ (normalized wave number)
β_r	$2\pi f$ = angular frequency of fluctuation
δ	boundary layer thickness
$\Delta e'$	instantaneous hot-wire a. c. output voltage component
ΔT_o	instantaneous a. c. fluid total temperature component
$\Delta(\rho U)$	instantaneous a. c. fluid mass-flow component
θ	momentum thickness of boundary layer $= \int_o^\delta \frac{\rho u}{\rho_\infty u_\infty} \left(1 - \frac{u}{u_\infty} \right) dy$
λ	fluctuation wavelength
μ	viscosity
ν	kinematic viscosity
ρ	density

A bar, such as in $\overline{(\Delta e')^2}$, denotes time averages

Subscripts

$( )_o$	stagnation conditions
$( )_\infty$	conditions at edge of boundary layer

I. INTRODUCTION

The problem of transition to turbulence of a fluid flow has for a long time attracted the attention and toil of both theoreticians and experimentalists. At hypersonic speeds the problem of transition is one of pressing importance, because the differences in skin friction and heat transfer between laminar and turbulent flow are large enough to alter radically the performance of a hypersonic aircraft or a long-range missile.

Of the various hypotheses put forth to describe the "triggering mechanism" of transition, one which has been steadily gaining ground is the so-called "small-disturbance" hypothesis. It states that within some range of the mean-flow parameters, certain infinitesimal disturbances found in the laminar part of the flow (whether wake, jet, or boundary layer) amplify as they progress downstream and eventually break up into the highly non-linear, random pattern which we identify as turbulence. The small-disturbance theory itself does not deal with the problem of turbulence; it merely examines whether and how disturbances amplify and damp in the laminar flow, and is therefore a theory of hydrodynamic stability.

The theoretical treatment of the stability of "parallel" flows with respect to small disturbances was formally initiated by Rayleigh[1]. The destabilizing role of viscosity for disturbances of a certain critical range of wavelengths was first put forward by Prandtl and Tietjens[2] and was first investigated for boundary layer flows by Tollmien[3]. Mathematical questions in the theoretical treatment were clarified by Lin[4, 5], who

also brought the earlier important work of Heisenberg[6] into clearer focus. Recently the stability of the boundary layer of a compressible fluid with heat transfer was investigated by Lees and Lin[7] and Lees[8]. All these authors used the equations of fluid motion in conjunction with a disturbance periodic in space and time. They showed that by retaining only the first order terms (for "small disturbances") one arrives at a system of linear homogeneous differential equations. For boundary layers with the proper boundary conditions an eigenvalue problem was produced, resulting in a prediction of stability or instability of a small disturbance, depending on its frequency and the local mean flow parameters.*

The small-disturbance theory of boundary-layer flows enjoyed its first success with the classic experiments of Schubauer and Skramstad[10], which showed the existence of the "laminar waves" of Tollmien, and which verified, both qualitatively and quantitatively, many of the prominent features of the theory. Soon afterwards Liepmann[11] reported the discovery of similar waves and studied their role in boundary layer transition on curved walls.

Other workers who concerned themselves directly with the laminar waves were Eckert[12], who studied briefly the stability of the free-convection layer, and Bennett[13] who recently repeated the Schubauer-Skramstad experiment. Finally, with the help of advanced instrumentation, the neutral stability boundaries as defined by the

---

* A very thorough survey of the historical and mathematical aspects of the stability theory of two-dimensional parallel flows appears in References 4, 5, and 9.

eigenvalue problem of laminar stability were recently discovered in supersonic flow as well. Laufer and Vrebalovich[14], in studying the flow over a flat plate at a Mach number of about 2, obtained data similar to that obtained by Schubauer and Skramstad at low speeds. It should be pointed out that all these experiments were identified as demonstrations of the small-disturbance theory and that their clarification of the transition problem itself was by no means complete.

Quite apart from the investigation of the laminar waves themselves, there have been a number of experiments aimed at demonstrating the "gross" (macroscopic) features of the small-disturbance theory of boundary layer stability. Such gross features include the effect on stability of the pressure gradient, heat transfer, surface smoothness, boundary layer suction, surface curvature, etc. Typically, Schubauer and Skramstad[10] found that a negative pressure gradient damps out the fluctuations and hence delays transition; Liepmann[15] that premature transition in incompressible flow is brought about by surface heating; and Pfenninger[16] that transition can be delayed by boundary layer suction. More recently, transition delay produced by surface cooling of smooth, slender cones was observed in supersonic flow by Czarnecki and Sinclair[17], Jack and Diaconis[18], Diaconis, Jack and Wisniewski[19], and also by Van Driest and Boison[20]. The results of these experiments again confirmed the validity of the small-disturbance theory and simultaneously provided the framework within which the relationship between hydrodynamic instability and transition to turbulence could be discussed.

The present experiment was undertaken in order to provide an

understanding of the stability of the hypersonic laminar boundary layer, and thus to encourage the extension of the laminar stability theory to higher Mach numbers. More specifically, the object of the experiment was to see whether there exist ranges of the defining parameters where small disturbances damp or amplify, to obtain information on the bounds of these ranges and to study the manner of amplification or damping. For this purpose the experimental set-up was limited to the simplest case of a smooth flat plate at zero heat transfer and pressure gradient, at a nominal Mach number of 5.80.

II. DEFINITION OF THE PROBLEM

The small disturbance theory shows that under the proper conditions a disturbance Q' of the form[5]

$$Q' = q(y)\ e^{i\alpha(x-ct)} \tag{1}$$

will amplify or damp in time depending on whether c_i, the imaginary part of c, is positive or negative. The condition

$$c_i = 0 = F(\alpha, Re, M, F)$$

is a direct result of the eigenvalue problem for "neutral" disturbances, where α is inversely proportional to the disturbance wavelength and Re is the Reynolds number; the latter is properly referred to the momentum thickness of the boundary layer. This relation shows that at every given Froude number F and Mach number M a "neutral stability boundary" can be drawn in the α-R_θ plane dividing it into a "stable" and "unstable" region. For flows of the boundary layer type, the Froude number can be excluded from the final form of the differential equations themselves. The "neutral" boundaries are therefore defined, for constant M, by

$$\alpha = f(R_\theta)$$

or by its equivalent

$$\frac{\beta_r \nu_\infty}{U_\infty^2} = g(R_\theta)$$

where β_r is the angular frequency of the disturbance, and ν_∞ and U_∞ are, respectively, the kinematic viscosity and the fluid velocity at the

edge of the laminar boundary layer of momentum thickness θ. The general shape of these neutral boundaries is pictured in Figure 1; the shape of the boundaries in the $\beta \nu_\infty / U_\infty^2 - R_\theta$ diagram is also similar. Two features of this so-called "stability diagram" are of immediate interest to the experimentalist, because they offer the simplest verification of the eigenvalue nature of the laminar stability theory.

First, observe that in equation (1), the form of the disturbance can be re-written so that it consists of a purely oscillatory part multiplied by an amplitude factor A where

$$A = q(y)\ e^{\alpha c_i t} \quad .$$

If the amplitude of a disturbance at constant frequency f is measured at some station 1 in the boundary layer and again at another station 2 downstream of 1, an amplitude variation

$$(A_2/A_1) \sim \exp \int_1^2 \alpha\ c_i\ dt$$

or

$$\ell n\ (A_2/A_1) \sim \int_{R_{\theta_1}}^{R_{\theta_2}} \frac{\beta_i \theta}{c_G}\ d\ R_\theta \qquad (2)$$

should be observed, where $\beta_i = \alpha\ c_i$ and c_G is the "group velocity"* of the disturbance given by

---

* For a discussion of group and phase velocities, see Reference 21, pp. 109-111.

$$c_G = c_r + a_\theta \left(\frac{\partial c_r}{\partial a_\theta} \right)_{R_\theta = \text{constant}}$$

These expressions illustrate the interdependence of time t and longitudinal location x (or R_θ) for the group of traveling waves, and hold strictly for the case where the disturbance frequency f measured at 1 is the same as that measured at 2. Thus, in traveling from station 1 to station 2 a disturbance of some particular frequency should damp or amplify monotonically, if the value of c_i (or β_i) between 1 and 2 is, respectively, everywhere negative ("stable region"), or everywhere positive ("unstable region"). If the neutral stability boundary lies between 1 and 2, then the disturbance amplitude variation is no longer monotonic in going from 1 to 2 but should exhibit a maximum and/or a minimum. In fact, if one follows the amplitude variation from 1 to 2 and observes a minimum, one can immediately suspect that the "lower stability branch" was crossed at that minimum. Similarly, a maximum would mean that the "upper neutral branch" was crossed; that is, that the disturbance passed from the unstable into the stable region.

It is obvious, therefore, that if discreetly bounded regions of stability or instability exist for the laminar hypersonic boundary layer as they do for the low-speed layer, then it should be possible to discover and chart them by finding the extrema in the streamwise amplitude distribution for disturbances of various given frequencies. This principle is illustrated in Figure 1. Suppose that a device recording the disturbance amplitude at frequency f only is moved downstream successively from R_{θ_1} to R_{θ_4}; in the stability diagram this procedure

corresponds to moving along the line f = constant from 1 to 4. The signal amplitude should decrease from 1 to 2, increase from 2 to 3 and again decrease from 3 to 4. If another frequency f' is chosen, then the minimum would be observed at some R_{θ_2}' different from R_{θ_2}, and the maximum at R_{θ_4}, different from R_{θ_3}. It should be kept in mind, of course, that all measurements should be carried out at the same relative distance y/δ above the solid surface, so that the factor q(y) of equation (1) will retain the same value from station to station.

The second important feature is that at sufficiently large Reynolds numbers the energy (or amplitude) spectrum measured at some particular streamwise location in the boundary layer should exhibit a maximum (a "peak") at some particular frequency. This statement is strictly correct if the initial disturbance energy distribution is fairly uniform with frequency. This property can be deduced by direct inspection of the stability diagrams of Tollmien and Schlichting and by considering the variation of the integrand in equation (1) for disturbances of different frequencies.

Suppose that the amplitude of two disturbances of frequencies f and f'' (Figure 1) are initially measured at location R_{θ_1} and are found to be the same; the amplitude of the same disturbances are next measured at a downstream location R_{θ_3}. Since the value of the integral in equation (2) depends not only on its limits but also on the range of the integrand between the limits, the amplitude of f'' and 3'' will be different from that of f at 3, and can easily be greater.* There will be, as a

---

* This fact is a consequence of the distribution of the lines c_i = constant $\neq 0$ (not shown on Figure 1). For example, see pp. 37-48, Reference 28.

matter of fact, some particular disturbance of frequency f' whose amplitude at R_{θ_3} is greater than that of f or f'' or of any other disturbance; in other words, at any streamwise location in the boundary layer there exists a continuous amplitude spectrum of disturbances over a wide frequency range, and this spectrum will exhibit a maximum ("peak") at some characteristic frequency; it is easy to realize how this peak frequency (and amplitude) will vary continuously with R_θ. The locus of the variation, called the "line of maximum amplification" is shown in Figure 1. One concludes that by measuring the disturbance energy (or amplitude) spectrum at various streamwise locations, one can draw conclusions about the stability problem by studying the existence of energy peaks and their frequency shift with R_θ.

These two steps in the investigation enable one to search for the neutral stability boundaries and the line of "maximum amplification" directly. Some secondary aspects of the theoretical problem were also investigated. The experimental method will now be described briefly.

III. THE EXPERIMENTAL METHOD

In discussing small disturbances in the boundary layer we have mentioned neither the origin nor the nature of these disturbances, beyond noticing that they are periodic or that they can be thought of as a sum of periodic components. As in the study of the stability of any physical system, the origin of disturbances is of no particular concern as long as it does not invalidate the assumptions and boundary conditions. In the present case we merely distinguish between "natural fluctuations", as those disturbances caused by free-stream turbulence, mechanical vibrations, leading-edge and surface irregularities, etc., and "artificial" or "induced fluctuations" as those disturbances of controllable magnitude and frequency, generated by a method to be described later.

In general, disturbances in the laminar boundary layer can exist in all three basic thermodynamic variables and in the velocity; thus the quantities Q' of equation (1) might be a density, a temperature, a pressure, or a velocity. Each of these has a different amplitude distribution factor $q(y)$ across the boundary layer but they all have the same wave number and wave velocity c, consistent with their functional interdependence. Thus they all exhibit the same variation of the damping factor c_i with α and R_θ. Simply stated, the eigenvalue problem has the same solution for all types if not for all magnitudes of two-dimensional disturbance. This fact is of paramount importance for the method of measurement, as will be explained below.

The simplest measuring device affording good spatial and temporal resolution for the study of boundary-layer stability is the

hot-wire anemometer. The operation of this instrument was first described theoretically by King[23], while others[24] developed it as a standard instrument for transient point measurements in fluid flows. More recently, Kovasznay[25, 26], Morkovin[27], and Laufer and McClellan[28] demonstrated its applicability to higher speed flows and paved the way for the present experiment. At supersonic Mach numbers above 2 or so the electrical power dissipated by the hot-wire anemometer is a function only of the wire Reynolds number Re and the temperature difference τ between the wire and the fluid surrounding it:

$$w = w(Re, \tau) \tag{3}$$

Therefore, for a hot-wire operating at constant current the fluctuating component of its voltage output is related to the fluctuations of the fluid mass-flow flux and total temperature about their corresponding mean values:

$$\Delta e' = -e_m \Delta(\rho U) + e_T \Delta T_o \quad ,$$

where e_m and e_T, the so-called "sensitivity coefficients", are functions only of mean quantities if the fluctuations are small. For purposes of measurement, the mean-square value of the voltage is obtained:

$$\overline{(\Delta e')^2} = e_m{}^2 \overline{\Delta(\rho U)^2} + e_T{}^2 \overline{(\Delta T_o)^2} - 2 e_m e_T R_{mT} \overline{\Delta(\rho U)}\,\overline{\Delta T_o} \quad , \tag{4}$$

where R_{mT} is the correlation coefficient between the mass-flow and the temperature fluctuation defined by

$$R_{mT} = \frac{\overline{\Delta(\rho U)\,\Delta T_o}}{\overline{\Delta(\rho U)}\;\overline{\Delta T_o}}$$

In the case of hypersonic flow it is natural to expect that high-frequency fluctuations in all flow variables will be present in the air stream. One could therefore proceed by measuring the mean-square voltage output of the hot-wire and then attempt to resolve it into the contributions from mass-flow fluctuations and from total temperature fluctuations, as in equation (4). However, insofar as the stability problem is concerned, this resolution is fortunately unnecessary. As stated earlier, within the limits of the small-disturbance theory, the neutral stability boundaries will be the same for all types of disturbance; and as the location (or R_θ) of the measuring device is changed, all three right-hand-side terms of Eq. (4) will experience the same percentage magnitude change. Therefore, in order to find the minima or maxima in the streamwise variation of the pressure, density, temperature, or velocity fluctuation amplitude distributions at some particular frequency, one simply attempts to find and record the corresponding extrema in the variation of the hot-wire voltage output $\Delta e'$, or its mean-square at that frequency. For the same reason, the spectral distribution of the energy of each type of disturbance at some location in the hypersonic boundary layer will all exhibit a maximum at some unique frequency, which will again correspond to the peak frequency of the total (unresolved) output of the hot-wire.

The experimental procedure then consisted of two distinct processes. The first, the "constant-frequency" process, consisted of studying the variation of the r. m. s. of the hot-wire output at each of various frequencies as the wire was moved along the boundary layer; the relative distance y/δ between the wire and the solid surface was

kept constant in order to insure the constancy of the coefficients e_m and e_T of equation (4) and of the value of q(y) in equation (1). The minima observed during these constant-frequency surveys then gave points on the lower neutral stability branch, and the maxima points on the upper branch. The second ("constant R_θ") process consisted of measuring the energy spectrum of the wire output in the laminar boundary-layer at a series of R_θ values, thereby obtaining evidence of the "line of maximum amplification" by studying the peaks in the spectrum.

IV. FACILITIES AND EQUIPMENT

A. Wind Tunnel

The present investigation was carried out in the GALCIT hypersonic wind tunnel (leg 1), which has been described in detail elsewhere (see Reference 29). The test section of this tunnel has a width of 5", a height of about 5-1/4", and a 29"-long test rhombus, as shown in Figure 2.

B. Flat Plate Models

Two different flat plate models were used in this investigation. The "survey" plate was used to study the stability of "natural" fluctuations, while the "siren plate" was used for generating artificial fluctuations and for studying their stability.

1. Survey Plate

This was the 26"-long flat plate with sharp leading-edge and smooth finish with which some experience had already been gained by Korkegi[30]. All injection and pressure-measuring orifices on this plate were sealed with solder in order to prevent leakage. With the aid of precision leveling methods, the plate was aligned within the test rhombus and at zero incidence as shown on Figure 2.

2. Siren Plate

This plate was externally almost identical to the survey plate above, measuring $\frac{1}{2}$" x 5" x 23" and tapering to a sharp leading edge.

The "siren" mechanism, which produces fluctuations of controllable amplitude and frequency, consists of pulsating air jets normal to the plate surface (Figures 3 and 4). A 4"-diameter thin brass siren disk is imbedded in the flat plate as shown. Along its circumference are drilled sixty regularly spaced holes, while another seven small (0.060" x 0.028") slits are drilled along a straight line normal to the flow direction in the cover plate shown, which is normally emplaced over the disk to make the top of the model a smooth, flat surface. The seven slits are spaced so that they either completely obscure or completely expose the holes in the siren disk as the latter rotates underneath. An air pulse is therefore injected into the flat-plate boundary layer for each 6^{o} of disk rotation.

Originally the plate was designed so that the line along which the slits were aligned was at a distance of 9.5" from the plate leading edge. Later all components were repositioned so that the slit line was 1.6" downstream of the leading edge. The disk is belt-driven from a drive pulley also imbedded in the plate, while the pulley itself is directly connected via the plate support to an 1/8-hp. AC series motor which is beneath the wind-tunnel floor. Because of the "gear ratio" involved the "siren frequency" in c.p.s. (i.e., the frequency of the pulsating jet) is numerically equal to twice the r.p.m. of the electric motor. Since the speed of the motor was controlled with a variable transformer, frequencies from about one up to about 30 to 40 kcps were attainable with a "drift" not exceeding 100 cps. The cavity containing the disk and drive pulley was airtight. However, a passage was constructed through the body of the plate bringing air from the outside of the tunnel to a point directly below the front part of the siren disk

and the seven injection slits. This flow of air and therefore also the magnitude of the injected disturbances could be regulated by a small valve.

Comments pertaining to the operation of the siren mechanism will be made in a later part of this work.

C. Hot-Wire Anemometer Probe

The hot-wire anemometer probe is pictured in Figures 5, 6, and 7. It consists of a long hollow brass strut which slides inside a brass sleeve which, in turn, is fastened to the test section actuator rods. The sleeve can be moved vertically above the plate surface; together with the streamwise motion of the strut, this mounting provides the hot-wire with two degrees of freedom (see Figure 5). The strut is moved with the aid of a rack-and-pinion arrangement and is manually driven from the outside of the wind tunnel by means of a flexible shaft.

Figure 6 shows the details of the detachable head which attaches to the fore part of the probe strut. The hot-wire element was soft-soldered on the tips of two heat-treated sewing needles which were in turn cemented in grooves on the surface of the head flange. The plane formed by these two needles met the plane of the plate surface at an angle of about 15° so as to eliminate local plate-probe interference. The thin electrical leads soldered to the blunt ends of the needles were led, through the hollow body of the probe head, to two miniature male connectors. The probe head was thus "plugged in" to a socket in the front of the probe strut and was steadied in place by a set screw. The electrical connection between the probe head and the outside of the

tunnel was maintained by a pair of very-small-diameter coaxial cables of a 50-ohm-per-foot impedance. The general overall arrangement of the probe in the test section is shown in Figure 8.

D. Electronic Instrumentation

The hot-wire resistance was measured by means of an accurate Wheatstone bridge of 0.05-ohm precision, although this figure could be still reduced by a factor of 100 with the aid of a precision potentiometer and an external galvanometer. The hot-wire was operated at constant current drawn from five 45-volt cells in series. The bridge and heating circuit are shown on Figure 9. The wire voltage fluctuation caused by the heating current fluctuation is, at most, about 300 times smaller than the fluctuation due to the wire resistance change.

Figure 10(a) shows the arrangement of the electronic devices necessary to record the fluctuations in the hot-wire output, and their characteristics. The pre-amplifier had a maximum gain of about 3,200 and an inherent noise output of about 10 millivolts at maximum gain, which is equivalent to the thermal agitation noise of a 600-ohm resistor, twenty times greater than the average value of the typical hot-wire resistance. The response curve of the amplifier is shown on Figure 10(b). A compensating amplifier was also provided to correct for the wire "thermal lag". The time constant of the hot-wire at any instant of its operation was determined by passing a square-wave signal at about 300 c.p.s. through the hot-wire. The response of the compensating circuit is shown on Figure 10(c) for various values of the wire time constant M'. Figure 10(d) shows the cumulative response

characteristics of the hot wire and the two amplifiers in series.

During the "constant frequency" work, the recording system was "tuned in" to the frequency of the fluctuation under study simply by rejecting all signals of frequencies above and below the one of interest; this "tuning" was accomplished with the aid of a band-pass filter, whose transfer function is shown in Figure 10(e). The relative magnitude of the voltage fluctuation were then measured with the aid of a vacuum thermocouple in series with a 92-ohm microammeter. A display-type wave analyzer was also found to be very useful in this connection*, as will be explained later.

During the "constant R_θ" work the filter was used merely to reject random electrical disturbances in the very low or very high frequency range. The energy spectrum was recorded with a harmonic wave analyzer and a thermocouple-microammeter combination.

E. Hot-Wire Technique

Platinum-rhodium (90 per cent Pt and 10 per cent Rh) hot-wires of 0.0001" diameter measuring from 0.02" to 0.03" in length were exclusively used in this work. Wires of 0.00005" diameter were tried but met with frequent structural failure, as did wires of 0.0001" diameter and aspect ratios of 1000 or more, while wires of diameter greater than 0.0001" were avoided because of inferior thermal lag characteristics. The wires were always held normal to the flow direction and parallel to the plate surface, so that they were sensitive

---

* The author is indebted to the Jet Propulsion Laboratory for the loan of the wave analyzer.

to the u' (streamwise) perturbation velocity component.

No novel problems requiring any special techniques in hot-wire anemometry were encountered. It was found expedient to anneal and pre-stretch the wire in the hypersonic stream itself; thus treated some wires were used for several tens of hours without any appreciable changes in electrical characteristics or any optically detected deterioration. No severe strain-gage effects[27] were encountered. Table 1 presents some of the pertinent operating conditions of the hot-wire.

Since this experiment involved only a comparison of disturbance amplitudes in space or in the energy spectrum, no need for calibrating the hot wires directly arose. The only occasion for measuring fluctuation amplitudes quantitatively presented itself during the measurement of the free stream turbulence level; in this case the experimental findings of Laufer and McClellan[28] took the place of relation (3) (page 11). Of more general interest from the standpoint of technique is whether a relation of the form of equation (4) can be derived from (3) for hypersonic flow in a manner similar to the low-speed case. Kovasznay[26] has pointed out that this process would be possible if the field around the hot-wire readjusts very rapidly to fluctuations in the flow parameters. In the present case the characteristic readjustment time, considered roughly equal to the ratio of hot-wire diameter to the fluid velocity, is less than a hundredth of a microsecond and thus very much smaller than any other characteristic time interval in the physical system.

V. THE FLOW FIELD

Before describing the hot-wire measurements in the hypersonic boundary layer, it is necessary to give an idea of the flow conditions prevailing in the wind tunnel. Two particular aspects are of interest: since the theory predicts that stability or instability depends on the local mean flow conditions only, it was desirable to study the steady-state boundary layer flow over the flat plate. Secondly, it was desirable to get an idea of the unsteady flow field in the air stream; i. e., the free-stream turbulence. These two items will now be described.

A. Boundary-Layer Flow over the Flat Plate Models

The laminar boundary layer over the survey flat plate at zero incidence at $M = 5.8$ was studied in some detail by Korkegi[30] and also by McMahon[31] and the author. The laminar boundary layer profiles obtained by using a total-pressure tube yielded the layer thickness δ and the momentum thickness θ along the center-line of the plate, shown in Figures 11 and 12. The former of these two thicknesses is the distance above the solid surface where the velocity becomes very nearly equal to the free stream velocity and was obtained from the boundary layer profiles by the method of Kendall[32]; the momentum thickness θ was obtained by numerical integration of the same profiles. On Figure 13 is plotted the momentum Reynolds number R_θ resulting from these measurements for $T_o = 225^\circ F$. Some pitot surveys were also taken off the centerline of the plate at various streamwise locations. The results indicated that spanwise distortions of the thickness of the

boundary layer, symmetrical about the plate centerline, grew along the plate edges, intensifying with downstream distance. This phenomenon was caused by the interaction of the plate boundary layer with the partly turbulent boundary layer of the test-section sidewalls, and its influence on the hot-wire measurements was difficult to assess by steady-state measurements alone.

The variation of the boundary-layer thickness δ and θ with x is not by itself sufficient to insure the rigor of the hot-wire measurements. It is also necessary to verify that there is an adequate resemblance between the prediction of the equations of the mean flow on which the small perturbation theory is based, and the actual mean flow over the flat plate models. This question can be most expediently checked by investigating the similarity among boundary layer profiles taken with a pitot tube at various x-locations. For constant Mach number the pitot pressure ratios should be independent of x or the stagnation conditions and should depend solely on y/δ. A series of such profiles taken along the survey plate centerline are shown on Figure 14 for three values of x and two of P_o. It definitely seems that similarity is preserved.

The boundary layer growth over the siren plate was also measured with flow conditions simulating those under which the presently described experiments were carried out. The siren disk remained stationary, but a small amount of air was injected at constant rate through the siren slits. The resulting thicknesses δ and θ for two sample x-stations and two stagnation pressures are shown in Figures 11 and 12. The agreement between these values and the values corresponding to the boundary layer on the survey plate is seen to be

good; Figure 13 was therefore used to obtain the Reynolds number R_θ as a function of P_o and x in reducing the experimental data.

Figure 13 also serves to illustrate the range of the parameter R_θ which was covered during the measurements. The highest utilizable stagnation pressure P_o is approximately 75 psig, while for stagnation pressures below about 30 psig the supersonic flow in the test section was "blocked" by the plate and the anemometer probe. On the other hand, the movable probe strut had a longitudinal "stroke" of 7.3" and could be positioned in order to cover two ranges; from x = 1.6" to 8.9", and again from 8.7" to 16". The choice of total temperature T_o of 225^o was governed by the minimum supply temperature necessary to sustain one-phase flow at a Mach number of 5.8 and by the maximum temperature allowable for the non-metallic components of the anemometer. As a result, the operating range of the anemometer is contained, in the $x - R_\theta$ diagram, within the parallelogram defined by the $P_o = 30$ and $P_o = 75$ isobars and the lines x = 1.6" and x = 16", with resulting minimum and maximum R_θ of 350 and 2,050, respectively. The wire could be raised to about 0.5" above the plate surface, covering the range y/δ from 0 to about 10 at the smallest R_θ, and thus measurements could be made in the free stream also, if desired.

The absolute magnitude of the boundary layer thickness also has direct bearing on the reliability of the procedure. Interference between the probe tip and the plate surface may cause local separation and the resulting positive pressure gradient should, at least theoretically, de-stabilize the laminar fluctuations, and thus produce an apparent

increase in the fluctuation amplitude.* For this purpose a specific measurement aimed at evaluating the probe-plate interference effect was conducted with the survey plate before its static pressure orifices (spaced 1.5" apart along the centerline) were sealed with solder. In the first instance the hot-wire was positioned one-half inch behind the orifice located at x = 9.5" and then traversed vertically across the boundary layer. The procedure was then repeated with the probe tip directly above the orifice; the resulting static pressure distribution is shown in Figure 15. It is seen that as long as the wire remains within the upper half of the layer, its proximity is felt only to the extent of 1 per cent of the local plate surface pressure level, and that the region of interference does not extend beyond one layer thickness ahead of the probe tip. The interference effect should be important for fluctuation wavelengths much smaller than the local layer thickness δ, but not for those much larger than δ, as was the case in the present experiment.

B. Free Stream Turbulence

In the preceding sections we discussed the technique of searching for the neutral stability branches by traversing the hot-wire along the boundary layer (at constant y/δ) and measuring its output at a series of pre-chosen frequencies. This "constant frequency" technique involves the tacit assumption that the rate at which disturbances from the external flow are introduced into the boundary layer ahead of the wire

---

* The streamwise steady-state static pressure distribution over the flat-plate models has been measured by Korkegi and appears on page 67 of his work (Reference 30).

is at all times smaller than the rate of amplification or damping of the sought-after laminar fluctuations. The technique of searching for the line of maximum amplification is also based on the assumption that the energy spectrum of the disturbances generated in the layer near the plate leading edge is uniform. To these one must add a third assumption, that the amplitudes of the fluctuations should be numerically much smaller than the corresponding mean-flow quantities. For a smooth, rigid flat plate the validity of these three assumptions hinges on the character of the time-dependent disturbances in the external flow.

For this reason the free-stream turbulence was investigated in the region of interest, namely in the region of the test-section which would be normally occupied by the flat plate boundary layer. First the spectral distribution of turbulence was measured and its comparative growth along the centerline of the test section was determined. Then an attempt was made to measure quantitatively the magnitude of the turbulence at one point along that line.

With the plate removed from the test section ("empty tunnel") the turbulence spectrum was recorded with the wire positioned normal to the flow at a total of eight locations along the test section of the centerline, covering the range from about 10" to about 23" downstream of the throat and for P_o = 30, 50, and 70 psig. The results for P_o = 50 are shown on Figure 16; note that in this instance and in this only the coordinate x refers to streamwise distance from the nozzle throat. The interesting features of these curves can be immediately singled out. There is a systematic monotonic increase of the fluctuation energy (as sensed by the hot wire between 0 and 50 kcps) with increasing

downstream distance, and a similar monotonic energy increase is also seen at each individual frequency. Further, an energy peak appears at about 10 kcps at the smaller x's and is intensified until it completely dominates the spectrum at the larger x's. Such an energy peak also appeared in the surveys at the total pressures of 30 and 70 psig.

The absolute level of the free-stream turbulence was measured at a distance of 17.5" from the nozzle throat. The procedure employed was to measure the wire output $\overline{(\Delta e')^2}$ at various wire temperatures (each temperature corresponding to different values of e_m and e_T in equation (4)), and then to compute the mass flow fluctuations and temperature fluctuations with the aid of the least-squares method. Figure 17 shows the variation of the sensitivity coefficients e_m and e_T with the overheating parameter A_w' as computed from the experimentally-determined variation of the hot-wire resistance with heating current;* the values of these coefficients have been corrected for the so-called "end effects" of the finite wire. The least-squares reduction of the data yielded values of the order of 0.4 per cent in both the mass-flux and the temperature fluctuation, almost independently of the tunnel supply pressure. In appraising these results the reader should be reminded that the agents generating the disturbances were by no means identified and that additional effort and care could perhaps reduce the turbulence level in the test section of the hypersonic wind tunnel.

The assumptions enunciated earlier in this section can now be

---

* The Jet Propulsion Laboratory courteously availed to the author its electronic computation facilities for this purpose.

re-examined in the light of the free-stream turbulence data. It would at first glance look as if the 0.4 per cent fluctuation intensity in the free stream is dangerously close to the broadly set 0.5 per cent limit for the linear stability theory to be valid.[33] However, the 0.4 per cent level found is really spread over a frequency range of about 100 kcps (the area under the curves in Figure 16), while the 0.5 per cent limit refers to the maximum allowable magnitude of a disturbance at some given frequency. Thus the free-stream disturbance energy contained in a narrow frequency band (say, between 20 and 25 kcps) will be one and possibly two orders of magnitude smaller than the allowable 0.5 per cent. As a matter of comparison, the 0.4 per cent level is about 10 times as large as that reported by Schubauer and Skramstad for their experiment, but of the same order as the free-stream turbulence level reported by Bennett.

Regarding the assumptions of uniformity of the disturbance spectrum in the free stream and of the constancy of the free-stream turbulence level along the tunnel centerline, conclusions from Figure 16 should be drawn with caution since the exact process of interaction of the hypersonic boundary layer with the time-dependent component of the external field is unknown. It is likely that some care should be exercised in the measurements in order to single out the effect of the increasing free-stream turbulence level with downstream distance. We will return to this consideration when discussing the hot-wire measurements in the boundary layer.

VI. MEASUREMENTS OF THE NATURAL FLUCTUATIONS

A. Measurements at Constant Frequency

The first measurement attempted was the study of the growth or decay of fluctuations which exist naturally in the laminar boundary layer; the survey plate was used for this purpose. The hot-wire was traversed along the layer at chosen constant values of y/δ and its output at a series of selected frequencies was recorded with the aid of the harmonic wave analyzer and the vacuum thermocouple-microammeter combination (see Figure 10(a)). Keeping y/δ constant as the hot-wire was moved stream-wise in increments of x was relatively simple, since the "hot" wire resistance R_w is a function only of the non-dimensional distance y/δ above the solid surface. At the beginning of each survey, therefore, R_w was recorded. As the probe was moved downstream by steps it was also raised a little, each time, so that the resistance-measuring galvanometer was again balanced at the previously set value of R_w. Through each survey, therefore, the wire was kept at constant resistance R_w and hence at constant value of y/δ.

Close to two hundred and fifty such surveys were recorded for various combinations of the tunnel supply pressure and the output frequency. Some typical data are singled out and shown in Figures 19 to 20. The abcissa of these graphs is the distance of the wire from the plate leading edge; the ordinate is the microammeter reading, which is proportional to the mean-square voltage fluctuation $\overline{(\Delta e')^2}$, and thence to the square of the fluctuation amplitudes or to the fluctuation energy (equations (2) and (4)) . Figure 19 shows the disturbance

amplitudes increasing monotonically with x for all frequencies below 8 kcps and decreasing monotonically for almost all frequencies above 10 kcps. Figure 20(a) shows the appearance of a maximum at a frequency of 45 kcps and Figure 20(b) a sequence of such maxima. Of the 250 surveys only a relatively small number, listed in Table 2, showed maxima, such as in Figure 20. The data of Table 2 have been reduced to the non-dimensional frequency $\beta \nu_\infty / U_\infty^2$ with the aid of Figure 18. The corresponding value of R_θ for each maximum was computed with the aid of Figure 13 using the P_o for the particular survey and the x-value at which the maximum appears. The y/δ values associated with these data range from about 0.7 to 0.9.

The non-dimensional frequencies $\beta \nu_\infty / U_\infty^2$ of each of the thirty-five points of Table 2 are plotted versus their corresponding R_θ (at the maxima) in Figure 21. These points seem to define a line which should be the upper neutral branch of the stability diagram, since it is the locus of the intensity maxima of the hot-wire output. Parenthetically, note that the data of Figure 19(a) (amplitude increasing with x) fall within the rectangle marked "unstable" in Figure 21, while the rectangle marked "stable" contains the data of Figure 19(b) (amplitude decreasing with x), consistent with the neutral boundary.

B. The Line of Maximum Amplification

As pointed out earlier, the amplitude spectrum of the natural fluctuations should exhibit a maximum (peak) when measured at any stream-wise location in the boundary layer. In the Schubauer-Skramstad experiment this "selectivity" property of the boundary layer was so

pronounced that the particular fluctuation inherently selected by the boundary layer for maximum amplification appeared as a pure sinusoidal oscillation of the wire output without any need for electronic filtering of any adjacent portion of the energy spectrum.

In searching for this selectivity property in the hypersonic boundary layer the survey flat plate was again employed, and the wire output spectrum was recorded for various combinations of the Reynolds number R_θ and the non-dimensionalized distance y/δ of the wire above the plate surface. At the typical values of this latter parameter the hot-wire overheat varied from about 0.35 to about 0.60 and its time constant lay above 0.7 milliseconds. The measurements were carried out originally with a harmonic wave analyzer having a range from 15 to 500 kcps and finally with another having a range from 0 to 50 kcps. After prolonged measurements at various ranges of the output frequency and the Reynolds number a series of energy peaks were discovered in the intervals from 0 to 5 kcps in frequency and 800 to 2000 in R_θ. The data are tabulated in Table 3 and also shown in Figures 22 and 23.

By far the most interesting feature of the energy spectra of Figure 22 is the absence of any completely predominant energy peak corresponding to the data of Reference 10 for incompressible flow. The energy peak is barely discernible at an R_θ of 880, although this lower limit is presumably strongly dependent on the free-stream turbulence level and other characteristics of the experimental environment. For larger values of x (or R_θ) the relative magnitude of the peak increases but certainly not in a manner permitting it, for

example, to be viewed on an oscilloscope screen without band-pass filtering. At the largest x-values attainable with the hot-wire probe traverse the peak is finally observed by an abrupt increase of the energy contained from 0 to 2 kcps in the spectrum. Figure 23* presents the points defined by the frequency-at-maximum-amplitude of the curves such as given in Figure 22.

It will be observed that no data taken at pressures P_o above 60 psig are presented in Figure 23. The energy peaks observed at 65 and 74 psig were at non-dimensional frequencies such that they fell far outside the locus of the points at the other pressures; those at 74 psig, in particular showed an energy concentration around 10 kcps and no decrease of the peak frequency with increasing R_θ. Earlier in this paper (Section V), it was pointed out that the spectral distribution of the free-stream turbulence exhibits a "peak" around 10 kcps in the spectrum. It is an unavoidable inference that the "maximum-amplification-line" data at 65 and 74 psig are greatly prejudiced by the free-stream turbulence.

A final point of interest concerns the value of y/δ at which the measurements just described were carried out. More specifically, one is interested in finding out how the amplitude peak at the fluctuation frequency which the boundary layer has selected for maximum amplification at some R_θ changes with y/δ. For this purpose the wire was held at some constant R_θ and was traversed across the boundary layer from the solid surface toward the free-stream in steps of

---

* The two solid curves on Figure 23 are the neutral branches to be discussed in Section VII.

about $\delta/5$ each. At each step the energy spectrum was recorded; six such spectra are shown in Figure 24. Since the current through the hot-wire was held constant, the reader should be reminded that the wire sensitivity varies considerably from spectrum to spectrum in this figure; however, the purpose here is to compare not the energy level from one spectrum to another, but the shape of each spectral distribution. Very near the plate there is no peak in the spectrum. As the wire is raised through the layer the peak, in this case at about 2.8 kcps, appears, becomes most discernible for values of y/δ between 0.6 and 1, persists briefly in the free-stream and again disappears for a y/δ of 1.34. The data points in Table 3 were indeed taken at y/δ values between 0.6 and 0.9.

C. Summary

At the conclusion of the work with the natural fluctuations encouraging evidence had been accumulated to the effect that the laminar hypersonic boundary layer observed, at least in a general way, the stability rules of the small-disturbance theory. A demarcation boundary between an unstable and a stable region had been found (Figure 21) and characteristic fluctuations at selected frequencies were also found and their dependence on R_θ was ascertained (Figure 23).

The amplification rates, however, were quite low and it was suspected that natural causes such as the free-stream turbulence, for example, might be concealing the detailed features of the stability diagram, and particularly the lower neutral branch.* For this reason the study of disturbances injected with the "siren" mechanism described in Section IV. B. 2 was undertaken. This study will now be described.

---

* This view was largely substantiated by a measurement which will be described later (cf. Figure 33).

VII. MEASUREMENT OF THE ARTIFICIAL FLUCTUATIONS

In utilizing the siren plate for the measurement of artificial fluctuations, care was taken to see that the amount of air injected did not cause premature transition. Just before any one constant-frequency survey was made the wire was located, say, at the middle of the x-range which was going to be covered, the siren was turned on, and the amount of injected air was gradually increased. Figures 25 and 26 show the effect of injection rate on the fluctuation amplitude and therefore, on the laminar nature of the boundary layer. For very small injection rates it was almost impossible to detect the induced fluctuation downstream of the slits. As the injection rate increased the energy peak corresponding to the siren frequency appeared and increased in magnitude. When some critical injection rate was reached the peak magnitude increased no further but an abrupt large increase of the wire output was noted over the entire frequency range; raising the injection rate further had no significant effect on the mean-square level of the wire output. This critical injection rate was, therefore, the one at which the layer became turbulent at the location of the wire. Knowledge of this rate enabled one to choose an injection rate appropriate for taking data and thus to estimate, even though roughly, the comparative magnitude of the fluctuation amplitudes. Generally, data were taken all at "sub-critical" rates, the guiding consideration being the appearance and clarity of the energy peak at the siren frequency. All artificial fluctuation data were taken by using the band-pass filter to suppress signals at all frequencies below and above that of the siren. From Figure 26 the reader can also obtain an idea of the relative magnitude

of the electronic noise, and the wire output in the boundary layer with and without the siren signal. The display-type harmonic wave analyzer proved invaluable in showing, instantaneously, the frequency and relative amplitude of the injected fluctuation.

In the original design of the siren plate the seven injection slits were located along a line 9.5" downstream of the plate leading edge, leaving a downstream distance of about 6.5" which could be traversed by the hot-wire probe. This range was further reduced since measurements directly over or closely downstream of the slits were not taken for fear that the geometry of the slit arrangement would affect the data. For this reason as soon as it was discovered that the injected artificial fluctuations could indeed be picked up by the hot-wire several inches downstream, the siren components were relocated so that the slits were at the $x = 1.6$" station downstream of the leading edge.

The results of the constant-frequency surveys appear in Figures 27 through 31. The value of y/δ was retained constant for each survey using the method described in the previous section. Figure 27 shows the amplitude variation of artificial fluctuations at 5.5 and 8 kcps as the wire is traversed along the boundary layer at constant y/δ; they both show minima in the amplitude variation. At close inspection one can notice the steadiness of the siren disk speed and also that at the largest downstream positions of the hot-wire and fluctuation seems to "feed" energy into a wider frequency band than at the lower x's. Figures 28, 29, and 30 show typical surveys at constant frequency exhibiting extrema in the amplitude variation. In almost all cases the variation of the location of the extrema (maxima or minima) with fluctuation frequency is

apparent. Table 4 shows the data in more detail. Note that the y/δ values again range from about 0.7 to about 0.9; as a rule the signals were very weak for y/δ much smaller than unity and disappeared rapidly once the probe was moved into the free-stream.

Although the siren mechanism could cover a frequency range up to about 40 kcps, no effort was made to make measurements above 30 kcps. As a matter of fact it was found that increasing use of the mechanism seemed to decrease the maximum angular speed of the siren disk, apparently because of friction developing in the bearings. For this reason the siren was not operated at frequencies much above 20 kcps for fear of damage, and most of the data above that frequency were taken by utilizing the second harmonic of the fluctuation excited by the siren. At times as many as four harmonics could be readily discerned in the wire output spectrum.

The results of the artificial-fluctuation study are shown in Figure 31 in the usual non-dimensional frequency plot. It is interesting to compare the stability diagram for the hypersonic boundary layer with similar findings at lower Mach numbers. (See Figure 32.) It is apparent that the general shape of the region of instability is preserved throughout the range of Mach numbers from 0 to 5.8. Another consistent trend appears to be the gradual decrease, with increasing Mach number, of the area enclosed by the neutral stability boundaries, at least above a certain low non-dimensional frequency. The shift of the neutral branches to much lower frequencies and longer wave lengths than those for the neutral branches at $M \simeq 0$ is also significant.

The data scatter of Figure 31 is of a still undetermined origin.

A glance at Table 4 suffices to verify that there seems to be no systematic effect of the supply pressure P_o on the scatter; nor does there seem to be an effect of y/δ and hence also of the wire sensitivity. The effect of the air injection rate, on the other hand, is difficult to estimate properly since it may be significant in two independent ways, namely by affecting the fluctuation amplitude and also by changing the boundary layer thickness. The latter effect is shown to be small in Figures 11 and 12. The effect of the amplitude of the artificial fluctuations was studied as follows: The ratio $\dot{m}/\dot{m}_c$ was obtained for each point on Figure 31, where $\dot{m}$ is the injection rate used for each survey and $\dot{m}_c$ is the critical rate for premature transition, as explained earlier. This ratio had, of course, a value smaller than unity for all points, and usually a value lower than 0.4. When the points on Figure 31 were re-plotted according to their corresponding magnitude of $\dot{m}/\dot{m}_c$, the data scatter remained practically unchanged. This result is particularly significant because it shows that in this "first-order" approach the experimentally determined neutral boundaries are relatively insensitive (within the order of the scatter) to changes in the fluctuation amplitude by as much as a factor of 3 to 4.

It is worth noticing that it became much easier to detect the lower neutral branch (minima in the hot-wire signal intensity variations) with the artificial fluctuations than with the natural fluctuations. Some light was shed on this point by a special test designed to bring forth a comparison of the "natural fluctuation" and the "artificial fluctuation" method. The top curve in Figure 33 (marked "siren on") shows a typical constant-frequency survey, in this case the variation of the hot-wire

output at 5.5 kcps. The second curve ("siren off") represents an identical measurement except that now the siren mechanism is stopped. Observe the large decrease in the signal intensity level and, more importantly, the fact that the intensity minimum at x = 4" is now almost impossible to detect. Next, the flat plate is removed from the wind-tunnel and the hot-wire is traversed through the same path as for the previous two measurements. When the wire sensitivity is adjusted to approximately the same value as for the two previous measurements, the streamwise intensity variation marked "empty tunnel" results. Observe how at locations near the leading edge (small x) the intensity level at 5.5 kcps is nearly the same in the free-stream as in the boundary layer. This fact may easily account for the inability to discover the lower neutral branch with the natural fluctuations.

The upper neutral branch found with the artificial fluctuations agrees very well with that found with the natural fluctuations at the lower non-dimensional frequencies but not so at the higher frequencies (see Figures 21 and 31). Although no effort was made to discover the cause of this difference, a comparison of the stream-wise growth of the free-stream turbulence with the data of Table 2 (the natural fluctuations) suggests a possible explanation. If the hot-wire output is for a moment thought to consist of the sum of the signal produced by the Tollmien-Schlichting fluctuations and the signal produced by the free-stream turbulence, then the effect of the latter would be to "displace" the upper neutral branch to the right of its natural position in the stability diagram. One can further maintain that this "displacement" will be more pronounced in those cases where the amplification rates of the laminar

fluctuations are small. If this explanation is correct, then Figure 31 suggests that the amplification rates at the higher non-dimensional frequencies are generally smaller than those at the lower frequencies; this statement is borne out by inspection of the curves on Figures 19, 20, 28, 29, and 30 and also by the stability theory at smaller Mach numbers.[10] A similar distortion of the upper neutral branch for the artificial fluctuations may have not occurred simply because the amplitude of these disturbances was larger than either that of the natural fluctuations or that of the disturbances in the free-stream.

VIII. THE CRITICAL LAYER

One of the features of the theory of boundary layer stability is that the phase velocity c_r of the laminar fluctuations is such that, for fluctuations "subsonic" relative to the free-stream,

$$1 - (1/M_\infty) < (c_r/U_\infty) < 1$$

so that for $M_\infty = 5.8$, we have

$$0.828 < (c_r/U_\infty) < 1$$

The point in the boundary layer where c_r is equal to the local gas velocity is called the critical point and the surface locus of these points over the flat plate is called the critical layer. On the basis of the comments made in Section II on the theory, the phase velocity also depends on the particular fluctuation frequency (or wavelength) and the local Reynolds number R_θ. However, if the theoretically predicted confinement of the critical layer within the upper 17 per cent of the boundary layer is true, then an approximation to the phase velocity becomes possible so that the fluctuation wavelengths can be computed. In the present instance it was assumed that $c_r = 0.9\ U_\infty$ = constant, which implies a maximum probable error of 10 per cent.

The above assumption was substantiated with the aid of a special test guided by the theoretical prediction that the amplitude factor q(y) of the laminar fluctuation has a maximum at the critical layer. Keeping the current constant, the hot-wire was traversed across the boundary layer and the change in the root-mean-square

output, integrated over all frequencies (corresponding to the area under each curve in Figure 24) was recorded. It was immediately noticed that the output increased rapidly as the wire approached the edge of the layer, came to a maximum at a y/δ of about 0.9 and then decreased to some constant value in the free stream, as shown on Figure 34. Considering that the curve defined in this figure has not been corrected for the rather rapid decrease of the wire sensitivity acorss the layer*, one sees that the energy concentration at the edge of the layer is indeed very pronounced. This behavior could not be explained on the basis of any assumed structural vibrations of the probe support or the plate model itself as can be deduced from inspection of Figures 19, 20, and 24 and other observations. It was concluded that the energy prominence was due to the cumulative effect of the maximum in the amplitude distribution factor $q(y)$ of the various fluctuations, and therefore that the value of y/δ at which this prominence appeared gave the position of the cirtical layer. From Reference 30 we can further deduce that at a y/δ of 0.9 the local flow velocity is about 0.98 of the free-stream velocity, which is within the expected 10 per cent error in the assumption $c_r = 0.9\ U_\infty$.

By using the approximation to c_r the fluctuation wavelengths can now be computed to the same degree of accuracy with the aid of the relation

---

* Inspection of Figure 17 and equations (67) of Reference 27 reveals that the sensitivity of the hot-wire to all types of fluctuations decreases rapidly as the wire is moved from the plate surface towards the free-stream.

$$\alpha_\theta = \frac{2\pi\theta}{\lambda} = \frac{R_\theta}{c_r} \left(\frac{\beta \nu_\infty}{U_\infty^2} \right) = 1.11 R_\theta \left(\frac{\beta \nu_\infty}{U_\infty^2} \right)$$

The result is shown on Figure 35, with the theoretical computations for M = 0 and M = 1.3 from Reference 8 also shown for comparison. With the aid of Figure 23 we observe that the fluctuations receiving maximum amplification in the range from R_θ = 1000 to 2000 have an α_θ of about 0.01. Since there is a difference of a factor of about 30 between the boundary-layer thicknesses δ and θ, the corresponding wavelengths are of the order of 20δ, or from 3 to 6 inches, that is much longer than the corresponding wavelengths for low-speed boundary layer flow.

IX. SUGGESTED EXTENSIONS OF THE WORK

Of the obvious possibilities for continuing and extending the stability work described in this paper, the following items of interest should be emphasized:

(1) The shape and location of the neutral stability boundaries for $M = 5.8$ at non-dimensional frequencies higher than those utilized in the present work

(2) Wavelength measurements of the laminar fluctuation in the layer

(3) Span-wise studies of the laminar fluctuations

(4) Study of the critical layer

(5) Study of the effect of geometry (e.g., nose bluntness, axial symmetry), pressure gradient, and heat transfer on the stability of the hypersonic boundary layer

(6) Study of amplification rates and transition, particularly as affected by the location of the critical layer.

X. CONCLUSIONS

The laminar boundary layer growing over an insulated flat plate at zero incidence in a hypersonic air stream has been investigated with the aid of a hot-wire anemometer. The main purpose of the investigation has been to see whether the hypersonic layer is hydrodynamically stable or unstable to small disturbances in the flow variables. The following results have been obtained:

(1) For certain ranges of the stagnation conditions and the frequency of the small fluctuations the boundary layer is stable, while for all other ranges of the same parameters it is unstable, in a manner resembling the theoretically and experimentally ascertained stability of boundary layer flows at lower speeds.

(2) The amplification rates observed are much lower than those observed at low speeds. Similarly, the characteristic fluctuations selected by the laminar layer for maximum amplification have a broad bandwidth, and hence are more difficult to detect than those at the lower speeds.

(3) The wavelengths of these characteristic fluctuations are of the order of twenty times the local boundary layer thickness δ, and of the order of 600 times the local boundary layer momentum thickness; they are therefore much longer than at low speeds.

REFERENCES

1. Lord Rayleigh: Scientific Papers, Cambridge University Press, Cambridge, Vol. 1, pp. 474-487 (1880); Vol. 3, pp. 17-23 (1887); Vol. 3, pp. 575-584 (1892); Vol. 4, pp. 203-209 (1895); Vol. 6, p. 917 (1913).

2. O. Tietjens: Zeit. Angew. Math. Mech., 5, 200-217 (1925).

3. W. Tollmien: Proceedings of the 3rd International Congress on Applied Mechanics, Stockholm, 1930, Vol. 1, pp. 105-108. Also, The Production of Turbulence, NACA TM 609, March, 1931; and General Instability Criterion of Laminar Velocity Distributions, NACA TM 792, April, 1936.

4. C. C. Lin: On the Stability of Two-Dimensional Parallel Flows. Part I - General Theory, Quarterly of Applied Math., Vol. III, No. 2, pp. 117-142, July, 1945.

5. C. C. Lin: On the Stability of Two-Dimensional Parallel Flows. Part II - Stability in an Inviscid Fluid, Quarterly of Applied Mathematics, Vol. III, No. 3, pp. 212-234, October, 1945.

6. W. Heisenberg: Ann. Der Physik, 74, 577-627 (1924).

7. L. Lees and C. C. Lin: Investigations of the Stability of the Laminar Boundary Layer in a Compressible Fluid, NACA TN 1115, Washington, D. C., September, 1946.

8. L. Lees: The Stability of the Laminar Boundary Layer in a Compressible Fluid, NACA Report 876, Washington, D. C., 1947.

9. C. C. Lin: The Theory of Hydrodynamic Stability, Cambridge University Press, London, 1955.

10. G. B. Schubauer and H. K. Skramstad: Laminar Boundary Layer Oscillations and Transition on a Flat Plate, NACA TR 909, Washington, D. C., 1948.

11. H. W. Liepmann: Investigations on Laminar Boundary Layer Stability and Transition on Curved Boundaries, NACA ACR No. 3H30, Washington, D. C., August, 1943.

12. E. R. G. Eckert: Interferometric Studies of Beginning Turbulence in Free and Forced Convection Boundary-Layers on a Heated Plate, Proceedings of the Heat Transfer and Fluid Mechanics Institute, Berkeley, California, 1949, (published by A. S. M. E.).

13. H. W. Bennett: An Experimental Study of Boundary Layer Transition, Kimberly-Clark Corp., September, 1953.

14. J. Laufer and T. Vrebalovich: Experiments on the Instability of a Supersonic Boundary Layer, External Publication No. 350, Jet Propulsion Laboratory, California Institute of Technology, Pasadena, California, August 27, 1956. Also, Proceedings of the 9th International Congress on Applied Mechanics, Brussels, 1957 (in press).

15. H. W. Liepmann and G. Fila: Investigations of Effects of Surface Temperature and Single Roughness Elements on Boundary Layer Transition, NACA TR 890, Washington, D. C., 1947.

16. W. Pfenninger: Experiments with Laminar Flow in the Inlet Length of a Tube at High Reynolds Numbers with and without Boundary Layer Suction, Northrop Aircraft, Inc., Hawthorne, California, May, 1952.

17. K. R. Czarnecki and A. R. Sinclair: An extension of the Investigation of the Effects of Heat Transfer on Boundary Layer Transition on a Parabolic Body of Revolution at a Mach Number of 1.61, NACA TN 3166, Washington, D. C., April, 1954.

18. J. R. Jack and N. S. Diaconis: Variation of Boundary Layer Transition with Heat Transfer on Two Bodies of Revolution at a Mach Number of 3.12, NACA TN 3562, Washington, D. C., September, 1955.

19. N. S. Diaconis, J. R. Jack, and R. J. Wisniewski: Boundary Layer Transition at Mach 3.12 as Affected by Cooling and Nose Blunting, Washington, D. C., January, 1957.

20. E. R. Van Driest and J. C. Boison: Experiments on Boundary Layer Transition at Supersonic Speeds, Journal of the Aeronautical Sciences, Vol. 24, pp. 885-899, December, 1957.

21. J. Valasek: Theoretical and Experimental Optics, John Wiley and Sons, Inc., New York, 1949.

22. A. M. O. Smith and N. Camberoni: Transition, Pressure Gradient and Stability Theory, Douglas Aircraft Co., Report No. ES-26388, El Segundo, California, August 31, 1956.

23. L. V. King: On the Convection of Heat from Small Cylinders in a Stream of Fluid, Philosophical Transactions of the Royal Society (London), Vol. 214, No. 14, Sec. A, pp. 373-342, 1914.

24. H. L. Dryden and A. M. Kuethe: The Measurements of Fluctuations of Air Speed in Turbulent Flows, NACA TR 320, Washington, D. C., 1928.

25. L. S. G. Kovasznay and S. I. A. Tornmarck: Heat Loss of Hot-Wires in Supersonic Flow, Bumblebee Report No. 127, The Johns Hopkins University, April, 1950.

26. L. S. G. Kovasznay: Turbulence Measurements, Article in Princeton Series Handbook on High-Speed Aerodynamics and Jet Propulsion, Vol. IX, pp. 213-276, Princeton, New Jersey, 1954.

27. M. V. Morkovin: Fluctuations and Hot-Wire Anemometry in Compressible Flows, AGARDograph No. 24, NATO, AGARD, November, 1956.

28. J. Laufer and R. McClellan: Measurements of Heat Transfer from Fine Wires in Supersonic Flows, Jet Propulsion Laboratory, California Institute of Technology, External Publication No. 315, December, 1955.

29. M. Eimer: Direct Measurements of Laminar Skin Friction at Hypersonic Speeds, GALCIT Hypersonic Wind Tunnel Memorandum No. 16, California Institute of Technology, 1953.

30. R. H. Korkegi: Transition Studies and Skin Friction Measurements on an Insulated Flat Plate at a Hypersonic Mach Number, GALCIT Hypersonic Wind Tunnel Memorandum No. 17, California Institute of Technology, July 15, 1954.

31. H. M. McMahon: An Experimental Study of the Effect of Mass Injection at the Stagnation Point of a Blunt Body, Ph. D. Thesis, GALCIT, Pasadena, California, June, 1958.

32. J. M. Kendall, Jr.: An Experimental Investigation of Leading-Edge Shock-Wave-Boundary Layer Interaction at M = 5.8, Journal of the Aeronautical Sciences, Vol. 24, pp. 47-56, January, 1957.

33. L. Lees: Instability of Laminar Flows and Transition to Turbulence, Consolidated-Vultee Aircraft Corp., Report No. ZA-7-006, San Diego, California, February 25, 1952.

TABLE 1

TYPICAL OPERATING CONDITIONS FOR THE HOT-WIRE ANEMOMETER

1.	material	Platinum 90 per cent Rhodium 10 per cent
2.	diameter	0.0001"
3.	length	0.02" - 0.03"
4.	aspect ratio	200 - 300
5.	Mach number	5.8
6.	wire Reynolds number Re_d (free stream conditions)	order of 1
7.	wire Nusselt number Nu_d* (free stream conditions)	order of 0.1
8.	resistance (equilibrium) R_e	30 - 40 ohms
9.	overheating parameter $\frac{R_w - R_e}{R_e}$	0 - 0.6
10.	overheating parameter $\frac{i}{2}\frac{1}{R_w}\left(\frac{\partial R_w}{\partial i}\right)$	0 - 0.6
11.	total pressure	28 - 75 psig
12.	total temperature	225°F
13.	dynamic loading	0.8 - 1.6 psi
14.	error in sensitivity coefficients due to "end effects"	5 - 10 per cent
15.	time constant M'	$0.2 - 1 \times 10^{-3}$ sec.
16.	maximum current through wire	about 10 ma.

* Estimated from Reference 28 for zero overheat

TABLE 2

EXTREMA IN THE AMPLITUDE VARIATION OF THE NATURAL FLUCTUATIONS (SURVEY PLATE)

No.	Run No.	P_o (psig)	f (kcps)	$\frac{\beta \nu_\infty}{U_\infty^2}$	Re/inch $\times 10^5$	R_θ (at i_{max})
1	958	45	20	2.46×10^{-5}	1.49	1240
2	958	65	8	0.74	1.99	1710
3	958	65	9	0.84	1.99	1660
4	958	65	10	0.93	1.99	1590
5	958	65	12	1.12	1.99	1530
6	999	30	9	1.49	1.12	970
7	999	30	10	1.65	1.12	970
8	999	30	12	1.98	1.12	970
9	999	40	9.5	1.37	1.36	1540
10	1014	45	12	1.60	1.49	1370
11	1014	45	14	1.87	1.49	1250
12	1014	45	16	2.13	1.49	1250
13	1014	45	18	2.40	1.49	1190
14	1014	45	20	2.66	1.49	1190
15	1014	45	22	2.93	1.49	1190
16	1014	45	24	3.20	1.49	1270
17	1014	45	22	2.93	1.44	1260
18	1014	45	24	3.20	1.49	1260
19	1014	45	26	3.44	1.49	1260
20	1014	45	28	3.73	1.49	1260
21	1014	45	30	4.00	1.49	1260
22	1014	45	32	4.26	1.49	1260
23	1014	45	34	4.53	1.49	1260
24	1008	55	12	1.27	1.74	1430
25	1008	55	14	1.48	1.74	1430
26	1008	55	16	1.70	1.74	1470
27	1008	55	18	1.91	1.74	1400
28	1008	55	20	2.12	1.74	1400
29	1055	28	26	4.52	1.07	600
30	1055	28	29	5.05	1.07	600
31	1057	55	33	3.50	1.74	1250
32	1057	55	36	3.82	1.74	1280
33	1057	55	39	4.14	1.74	1190
34	1057	55	42	4.45	1.74	1175
35	1057	55	45	4.77	1.74	1175

TABLE 3

MAXIMUM-AMPLIFICATION-LINE DATA (NATURAL FLUCTUATIONS)

Run No.	P_o (psig)	x (inches)	R_θ	$\beta \nu_\infty / U_o^2$ (at i_{max})
955	35	11.5	1070	0.62×10^{-5}
955	35	14	1200	0.59
955	35	16.5	1300	0.44
955	55	11	1400	0.53
955	55	12.9	1510	0.42
955	55	14.7	1620	0.24
955	55	16.5	1720	0.21
958	28	12	990	0.78
958	28	14.1	1080	0.66
958	28	16.5	1180	0.52
958	45	11	1230	0.74
958	45	12.7	1350	0.61
958	45	14.6	1430	0.58
958	45	16.5	1530	0.37
959	60	16.5	1800	0.25
961	40	16.5	1400	0.40

TABLE 4

EXTREMA IN THE AMPLITUDE VARIATION OF THE ARTIFICIAL FLUCTUATIONS (SIREN PLATE)

No.	Date	P_o (psig)	y/δ	f (kcps)	R_θ (at i_{min})	R_θ (at i_{max})	$\frac{\beta \nu_\infty}{U_\infty^2}$
8	12-4-57	60	.9	5	--	1870	$.49 \times 10^{-5}$
10	12-4-57	70	.9	2.4	--	1950	.21
18	12-5-57	50	.7	2.5	--	1700	.28
19	12-5-57	50	.7	4.5	--	1600	.51
20	12-5-57	40	.7	11.2	1100	--	1.52
21	12-5-57	40	.7	11.6	--	1250	1.58
22	12-5-57	40	.7	14.8	--	1190	2.01
23	12-5-57	50	.7	9.5	--	1420	1.08
24	12-5-57	50	.7	14	--	1380	1.60
25	12-5-57	50	.7	20	--	1290	2.28
26	12-5-57	60	.7	10.5	--	1620	1.04
27	12-5-57	60	.7	14.4	--	1450	1.42
28	12-5-57	60	.7	18	--	1370	1.78
29	12-5-57	70	.7	10	--	1700	.87
31	12-5-57	70	.7	18.5	--	1500	1.61
33	12-6-57	30	.7	13	--	1060	2.14
37	12-6-57	30	.7	7.7	--	1080	1.27
42	12-6-57	40	.7	9	--	1170	1.22
32	12-6-57	40	.7	6	--	1190	.82
44	12-6-57	40	.7	12.8	--	1250	1.74
45	12-6-57	40	.7	2.8	--	1200	.38
47	12-6-57	60	.9	7.5	--	1270	.74
48	12-7-57	60	.7	2.7	910	--	.27
49	12-7-57	60	.7	7.2	1060	--	.71
50	12-7-57	50	.7	2	1070	--	.23
51	12-7-57	50	.7	3.5	1040	--	.40
52	12-9-57	40	.7	2	820	--	.27
53	12-9-57	40	.7	7.5	880	--	1.02
54	12-9-57	40	.7	16	700	1070	2.17
55	12-9-57	40	.7	19	620	1000	2.58
56	12-9-57	35	.7	16	730	--	2.35
57	12-9-57	35	.7	20	650	--	2.94
59	12-9-57	40	.7	10.6	820	--	1.44

TABLE 4 -- continued

No.	Date	P_o (psig)	y/δ	f (kcps)	R_θ (at i_{min})	R_θ (at i_{max})	$\frac{\beta \nu_\infty}{U_\infty^2}$
60	12-9-57	40	.7	10.2	700	--	1.39×10^{-5}
61	12-9-57	40	.7	13	730	--	1.77
63	12-9-57	30	.7	9.8	680	--	1.62
64	12-9-57	30	.7	16.2	630	--	2.67
65	12-9-57	30	.7	19.5	610	--	3.22
66	12-9-57	35	.7	1.8	830	--	.26
69	12-9-57	30	.7	5	750	--	.83
71	2-24-58	50	.8	15	1240	--	1.73
72	2-24-58	50	.7	19	1190	--	2.19
82	2-27-58	50	.7	15	1060	800	1.73
83	2-27-58	50	.7	20	960	830	2.30
84	3-3-58	30	.9	15	--	735	2.46
85	3-3-58	30	.9	20	780	600	3.28
86	3-3-58	30	.9	25	685	570	4.10
87	3-3-58	30	.9	30	660	570	4.92
88	3-4-58	40	.9	5.5	--	660	.75

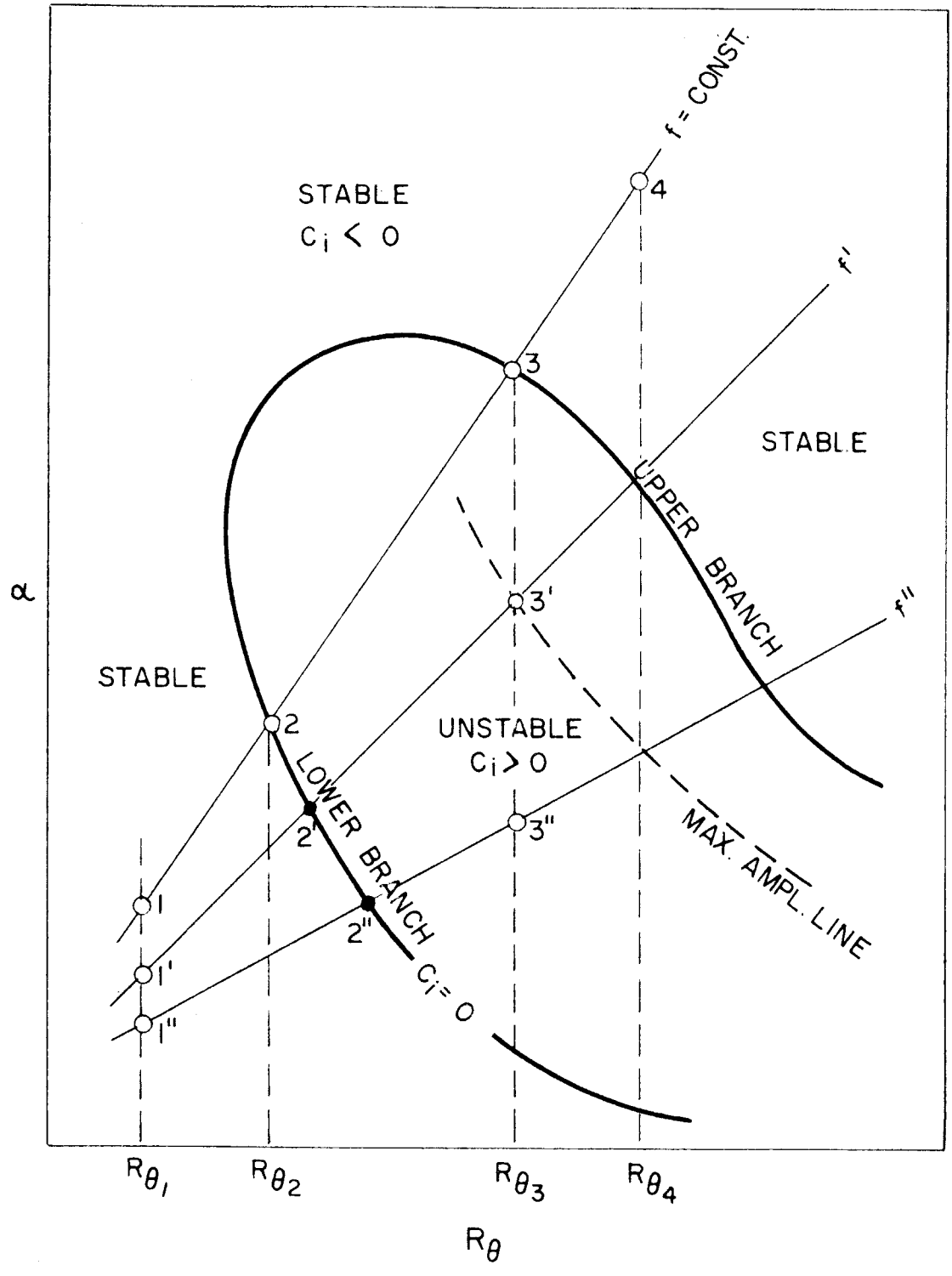

FIGURE 1 – SCHEMATIC PRESENTATION OF THE STABLE AND UNSTABLE REGIONS FOR A LAMINAR BOUNDARY LAYER

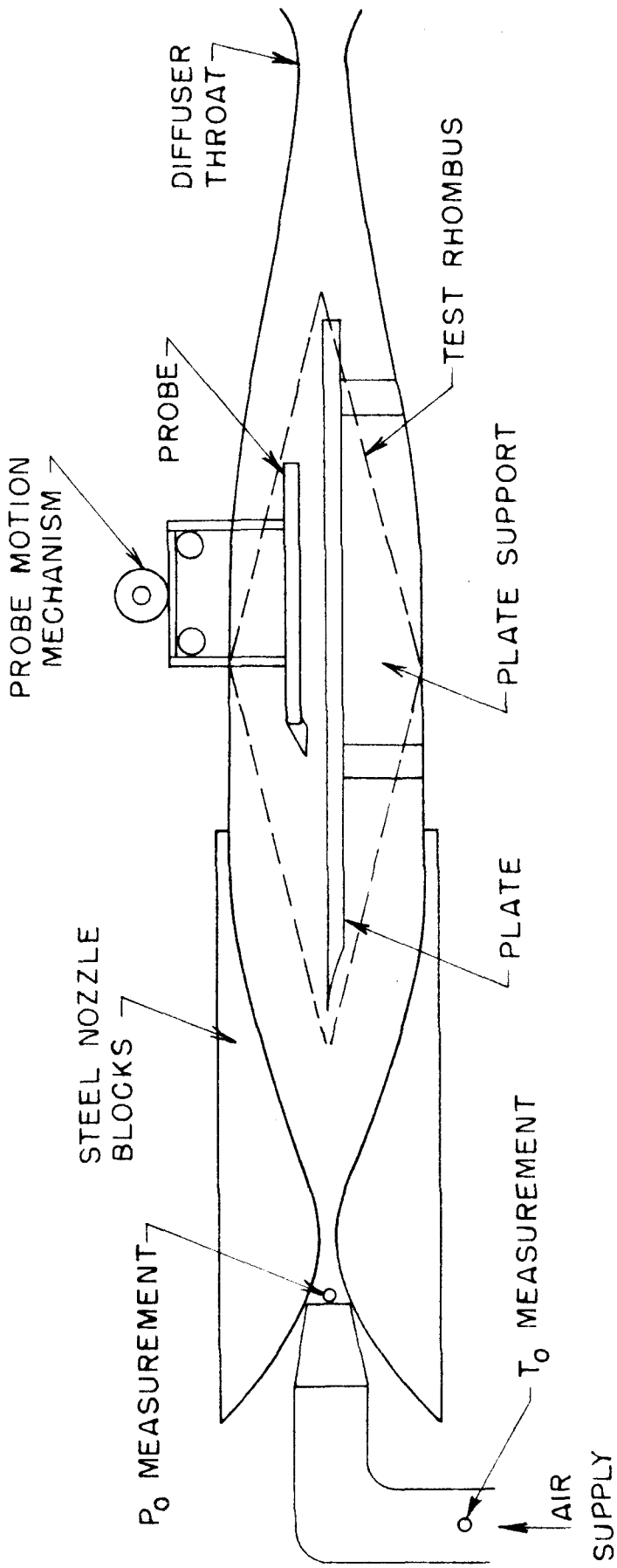

FIG. 2 – SCHEMATIC DIAGRAM OF GALCIT LEG I HYPERSONIC TUNNEL TEST SECTION SHOWING FLAT PLATE AND PROBE INSTALLATION

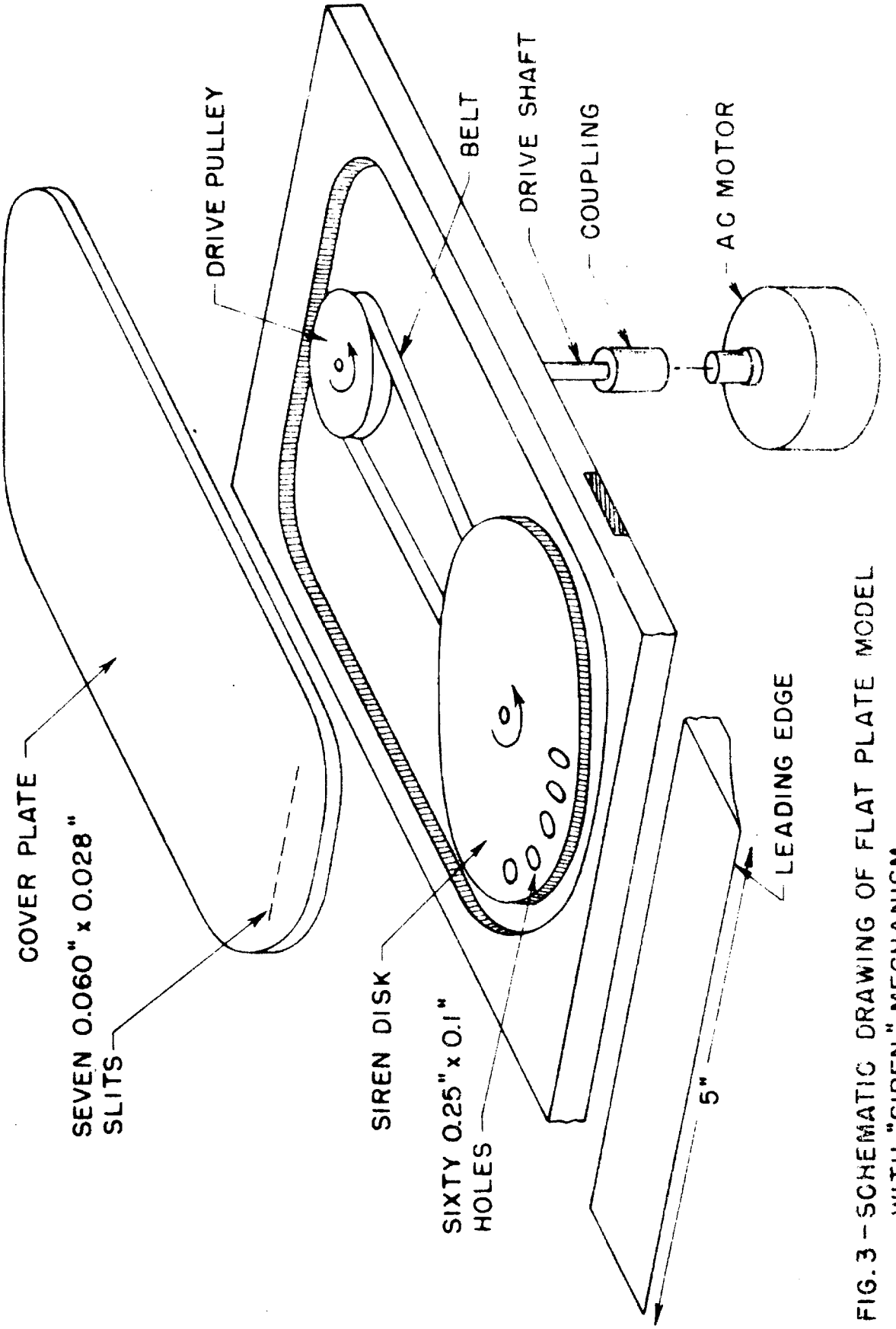

FIG. 3 - SCHEMATIC DRAWING OF FLAT PLATE MODEL WITH "SIREN" MECHANISM

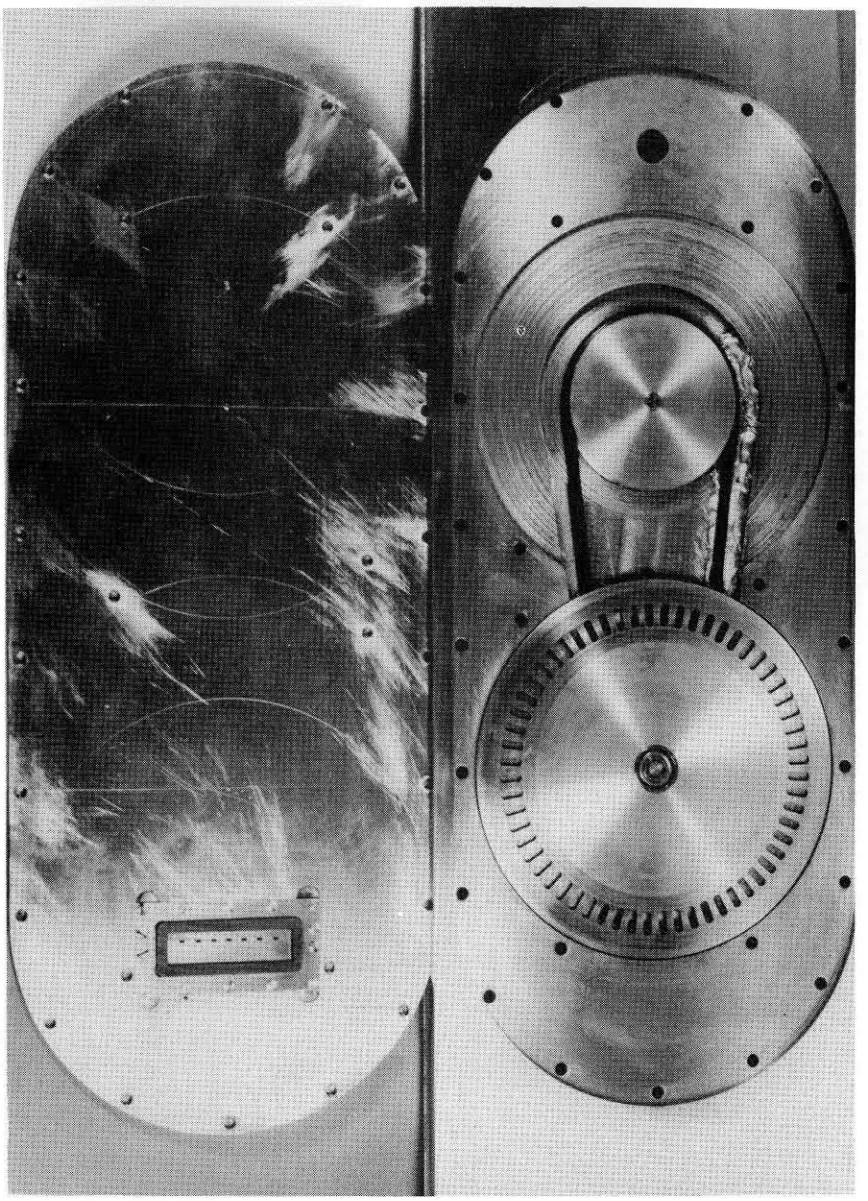

FIGURE 4

PHOTOGRAPH OF THE SIREN PLATE (RIGHT)
WITH THE COVER PLATE (LEFT) REMOVED

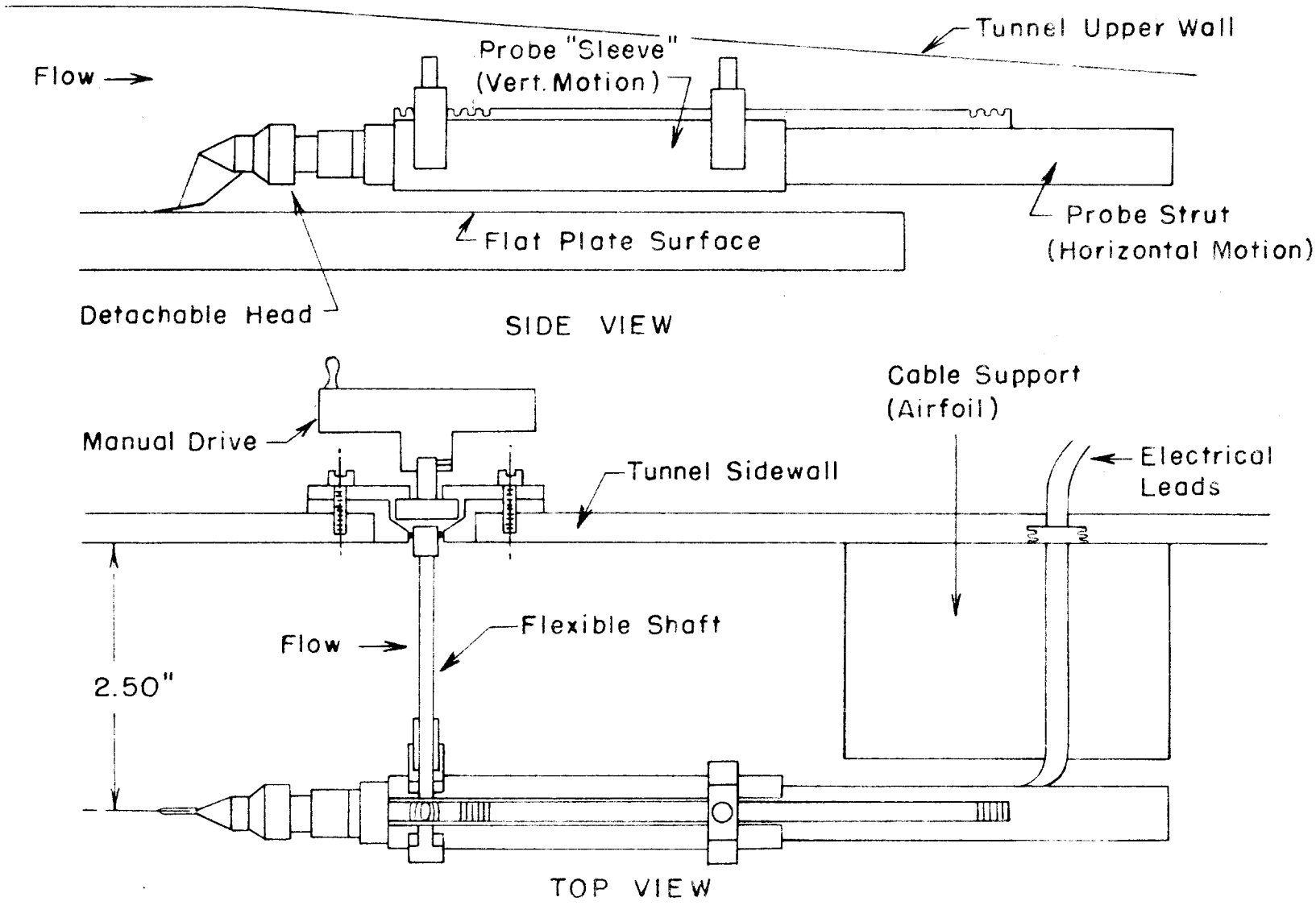

FIG. 5 – HOT-WIRE ANEMOMETER PROBE AS INSTALLED IN LEG I OF THE HYPERSONIC TUNNEL

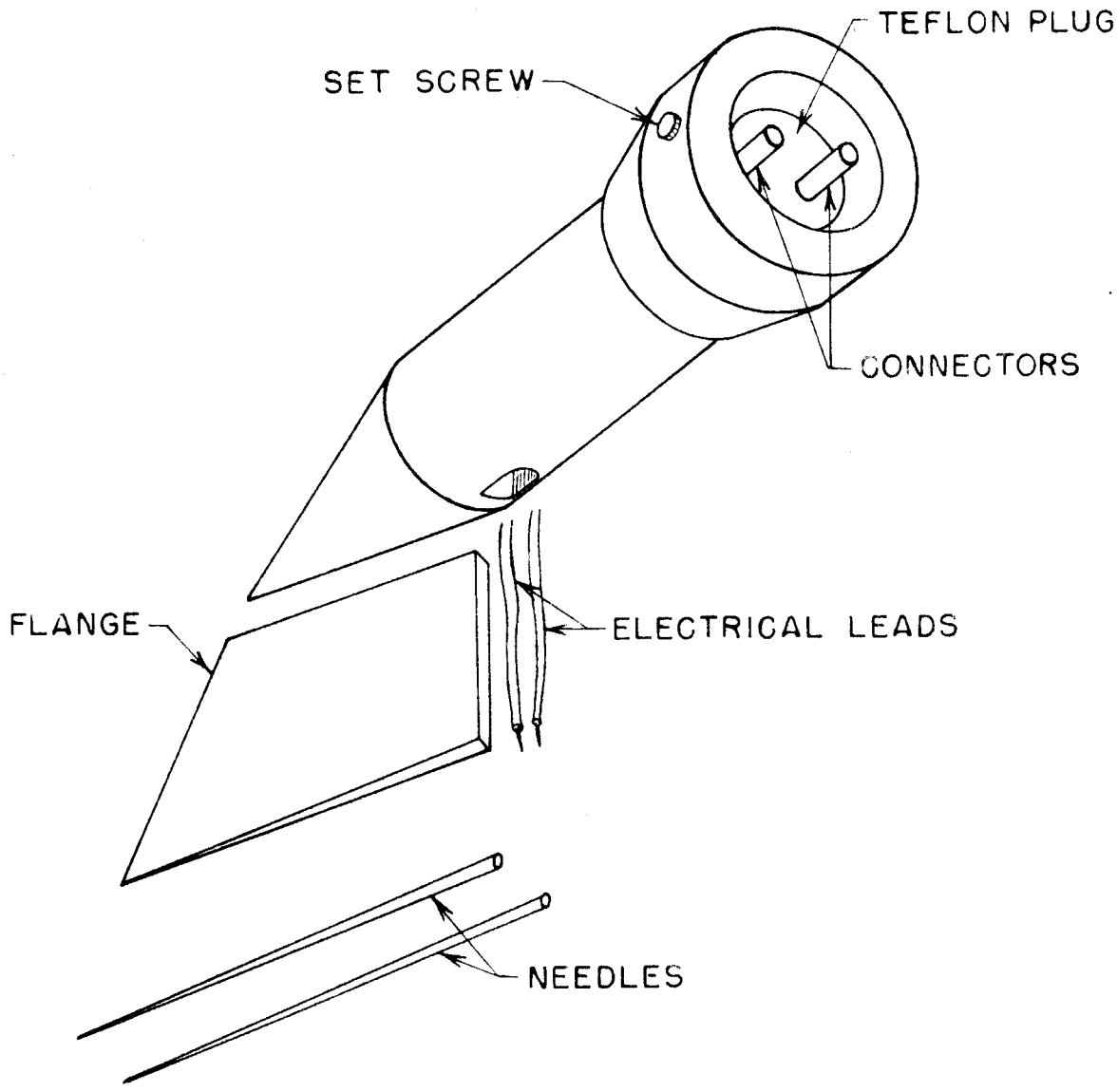

FIG. 6 – EXPLODED SCHEMATIC VIEW OF THE HOT-WIRE ANEMOMETER PROBE HEAD

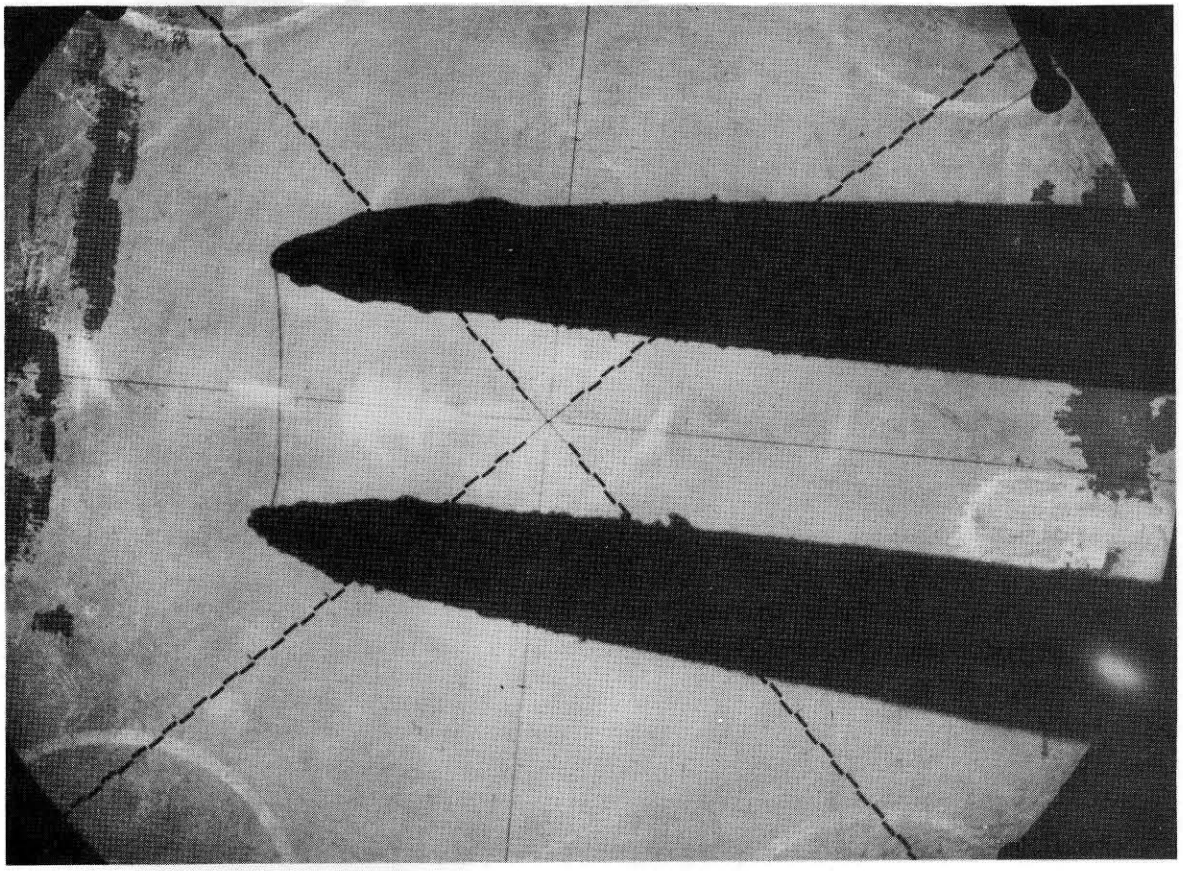

FIGURE 7

MICROCOMPARATOR PHOTOGRAPH OF A 0.0001"-DIAMETER HOT-WIRE MOUNTED ON THE PROBE NEEDLE TIPS

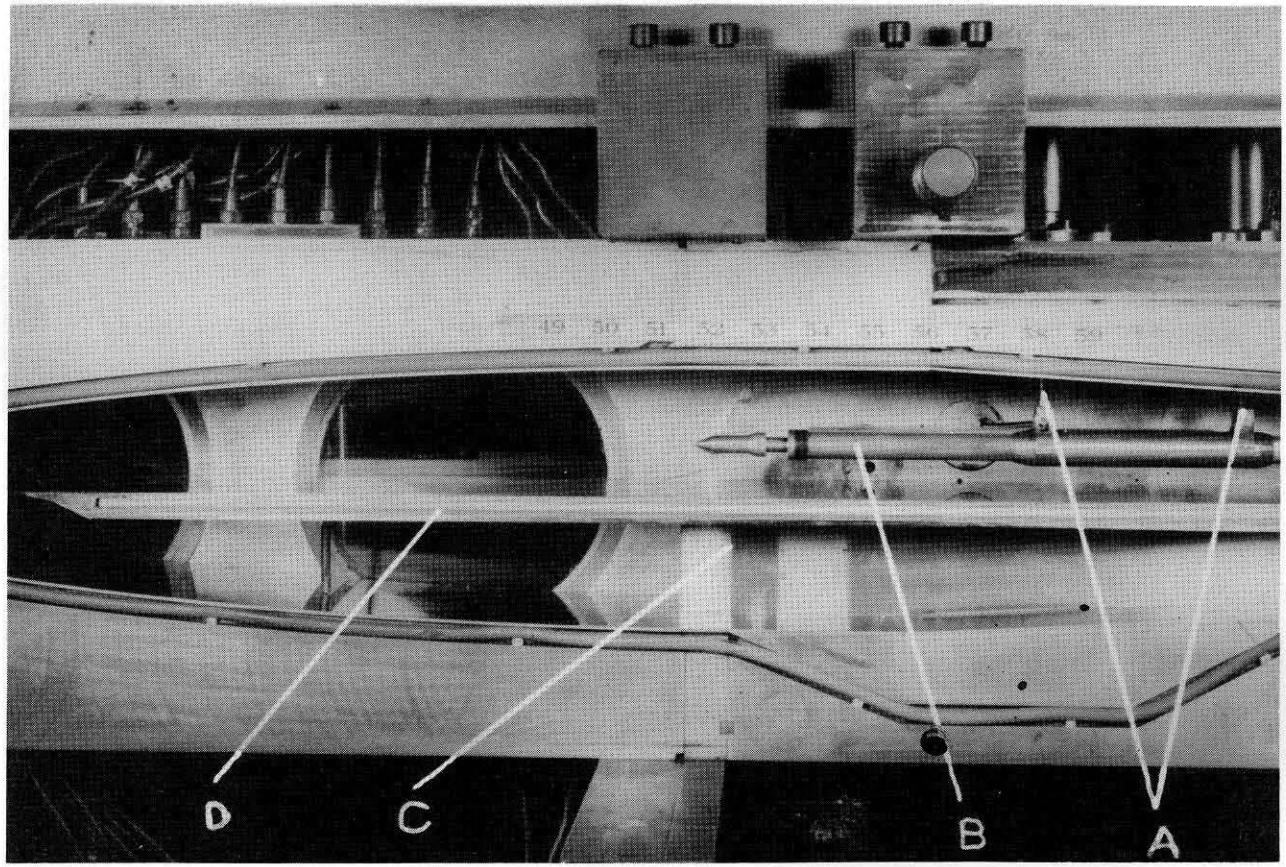

FIGURE 8

PHOTOGRAPH OF THE TEST SECTION OF THE GALCIT LEG 1 HYPERSONIC TUNNEL SHOWING: A. PROBE SLEEVE SUPPORTS; B. PROBE STRUT; C. FLAT PLATE SUPPORT; D. FLAT PLATE MODEL

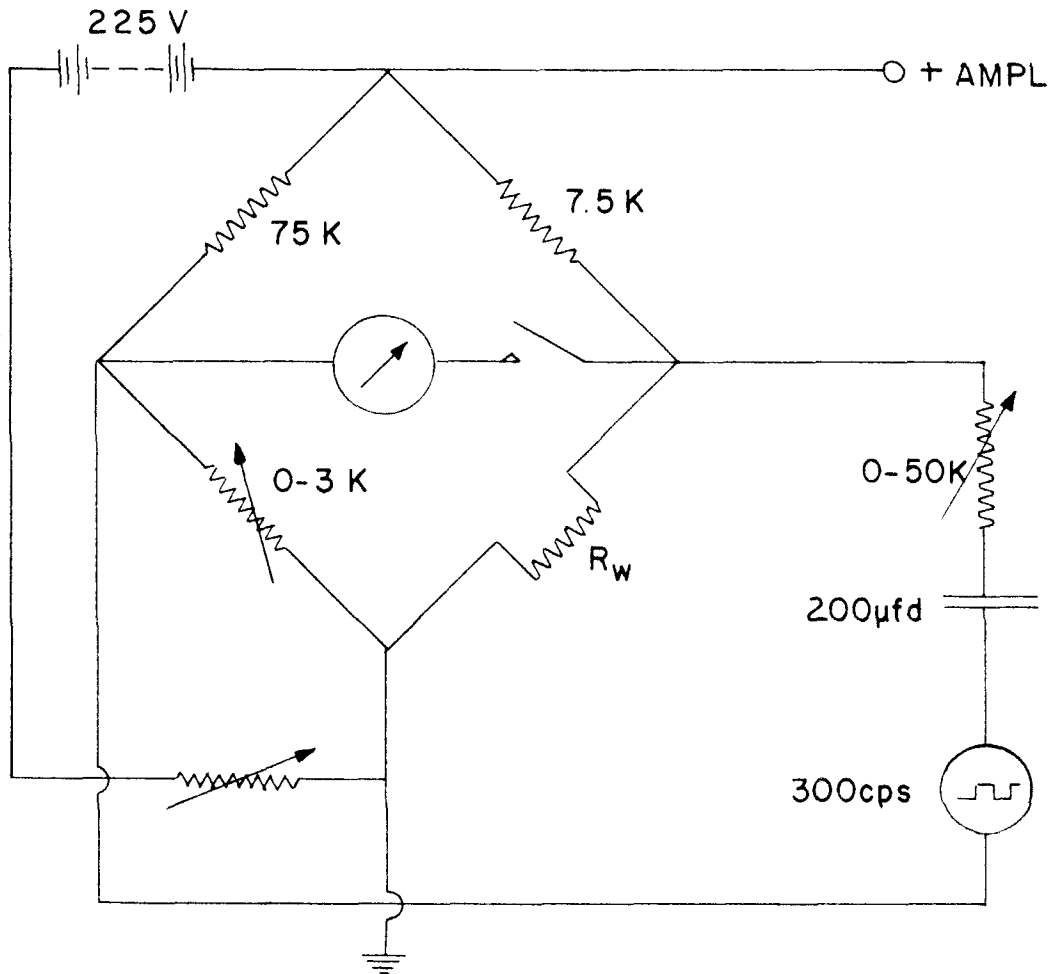

FIGURE 9 - WHEATSTONE BRIDGE, HEATING CIRCUIT AND SCHEME OF COMPENSATION FOR HOT-WIRE R_w THERMAL LAG

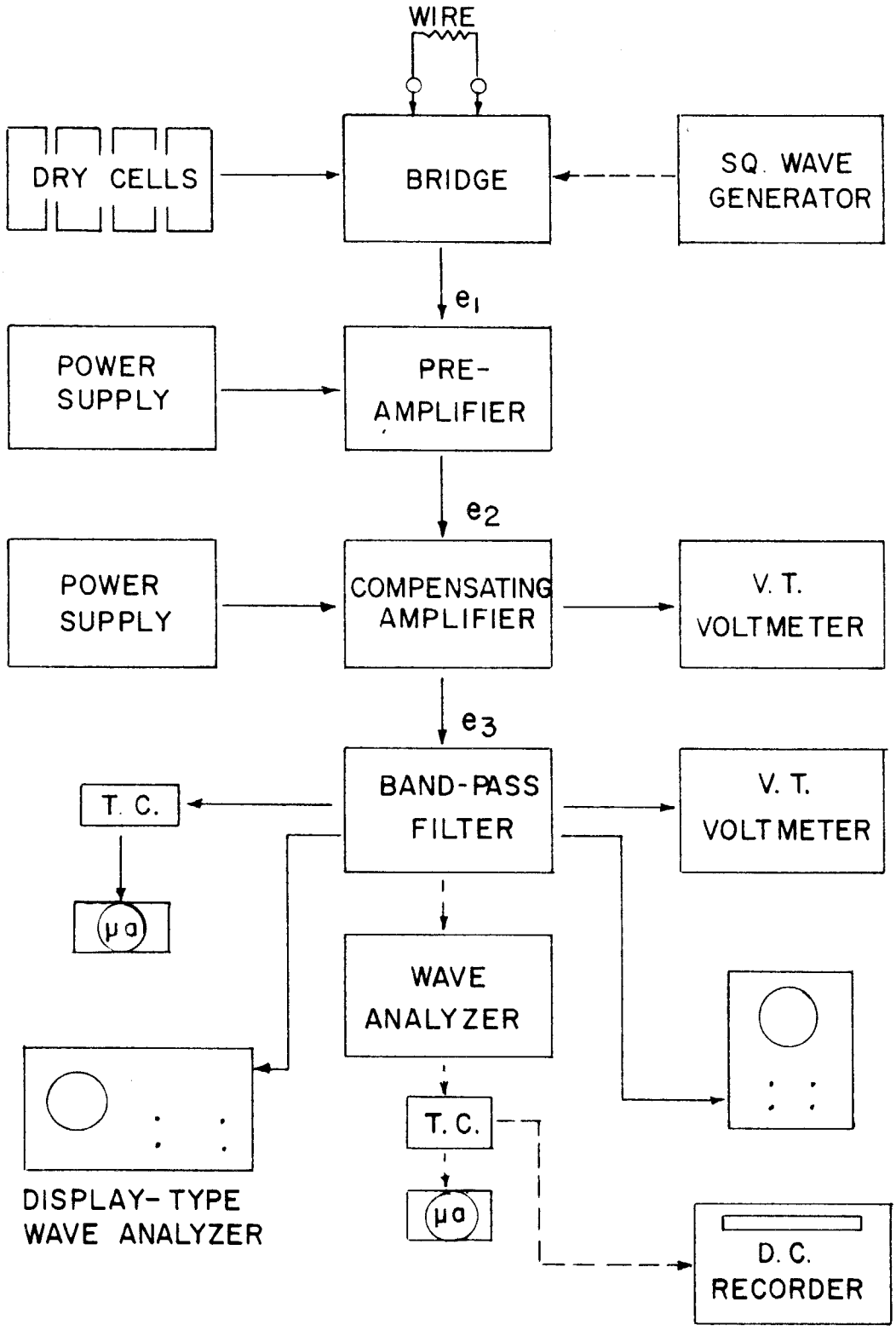

FIG. 10a-BLOCK DIAGRAM OF ELECTRONIC INSTRUMENTATION FOR HOT-WIRE MEASUREMENTS

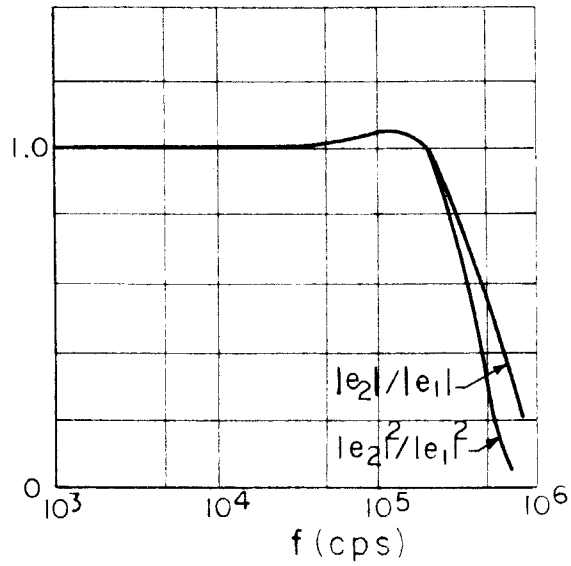

FIGURE 10b – FREQUENCY RESPONSE CURVE OF THE PREAMPLIFIER

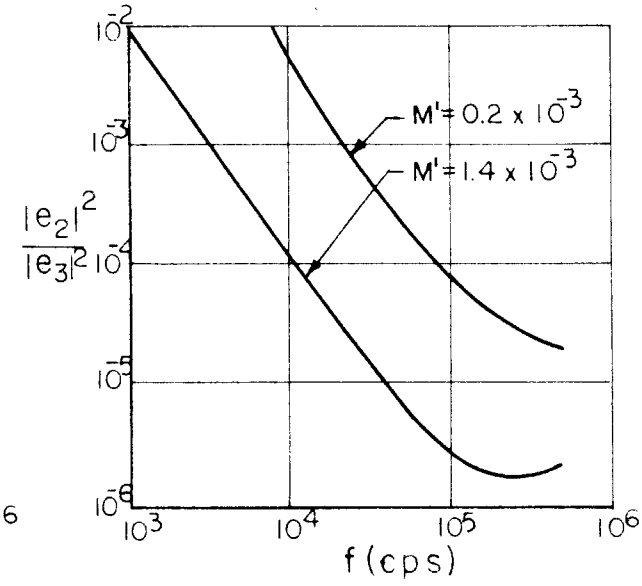

FIGURE 10c – FREQUENCY RESPONSE CURVE OF THE COMPENSATING AMPLIFIER

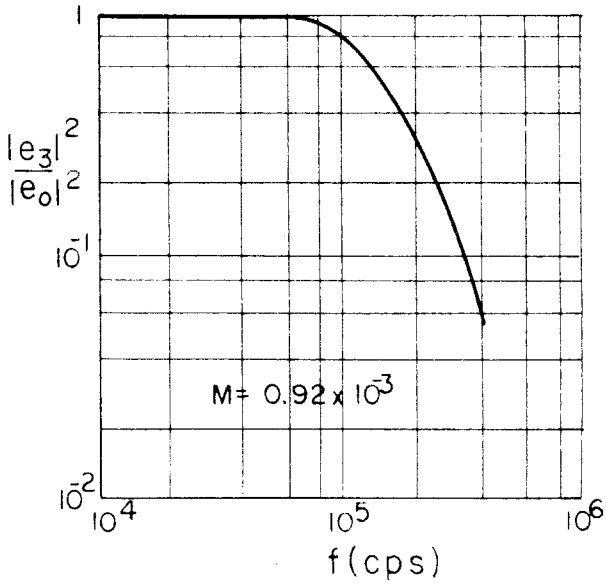

FIGURE 10d – TYPICAL OVERALL FREQUENCY RESPONSE OF THE SYSTEM WIRE – PREAMPLIFIER – COMPENSATING AMPLIFIER

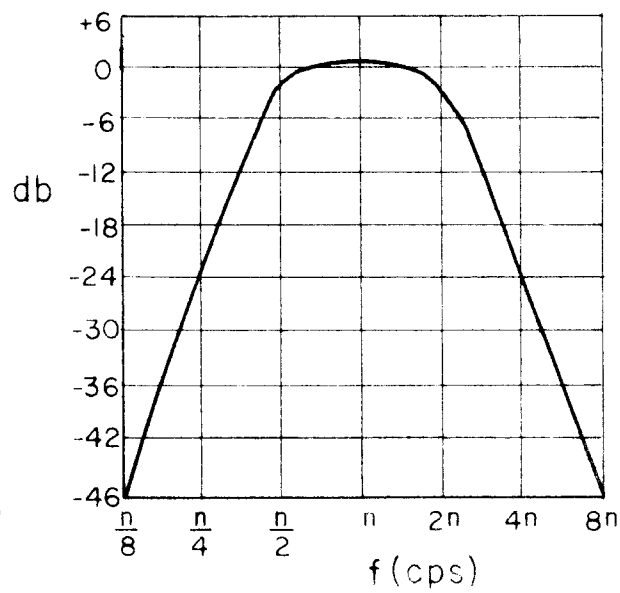

FIGURE 10e – RESPONSE OF THE BAND-PASS FILTER REJECTING ALL FREQUENCIES ABOVE AND BELOW n

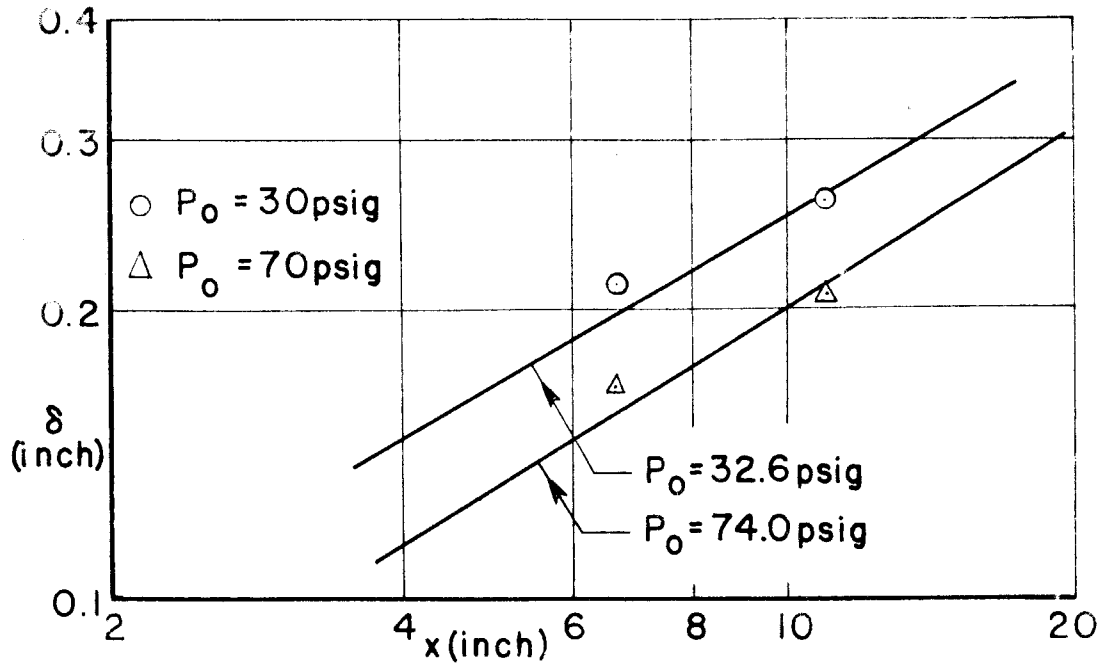

FIG. 11 — BOUNDARY LAYER GROWTH ON SURVEY PLATE (SOLID LINES) AND SIREN PLATE (POINTS) ALONG CENTERLINE

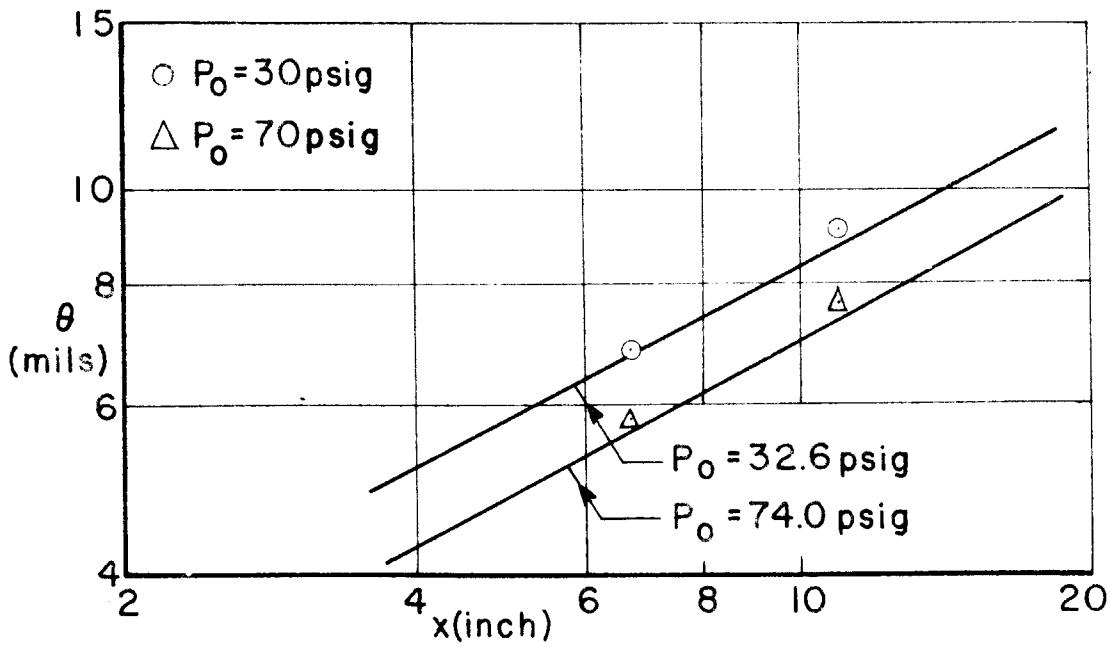

FIG. 12 - MOMENTUM THICKNESS GROWTH ON SURVEY PLATE (SOLID LINES) AND SIREN PLATE (POINTS) ALONG CENTERLINE

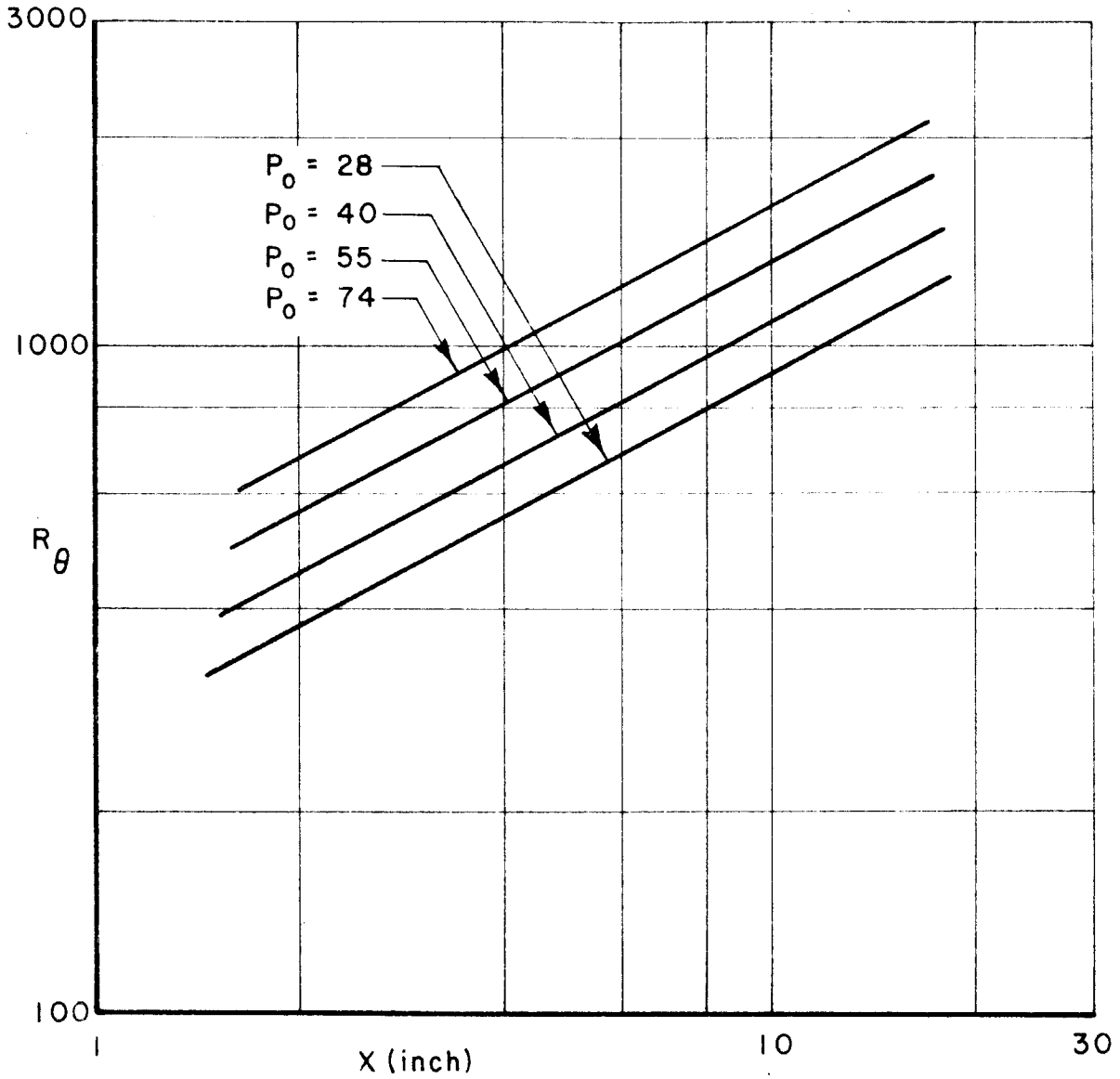

FIG. 13 – VARIATION OF REYNOLDS NO. R_θ FOR A FLAT PLATE AT ZERO INCIDENCE AT M = 5.8, T_0 = 225°F BASED ON FIGURES 11 AND 12

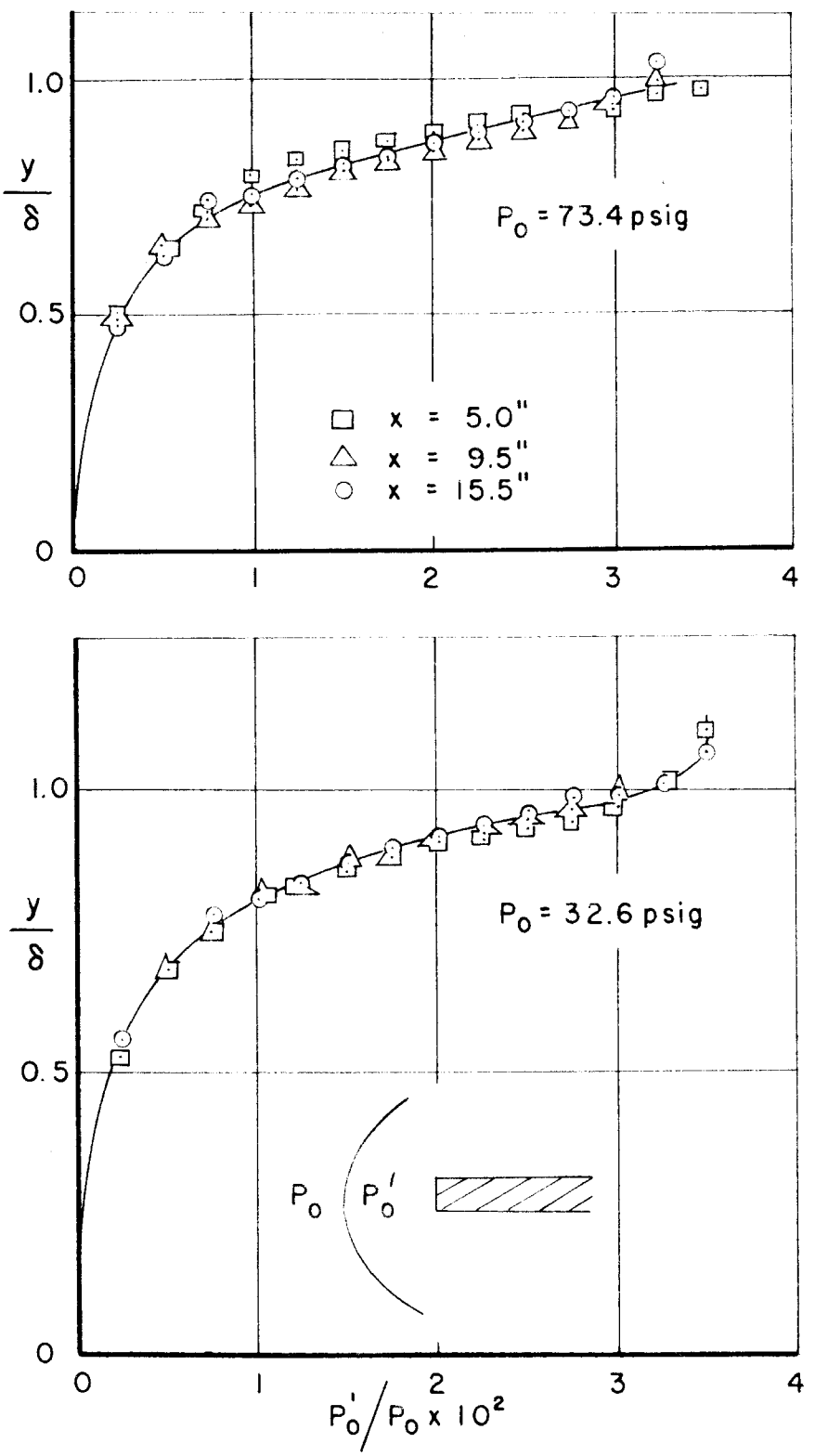

FIG. 14 – SIMILARITY OF BOUNDARY-LAYER PROFILES ALONG THE CENTERLINE OF THE SURVEY PLATE

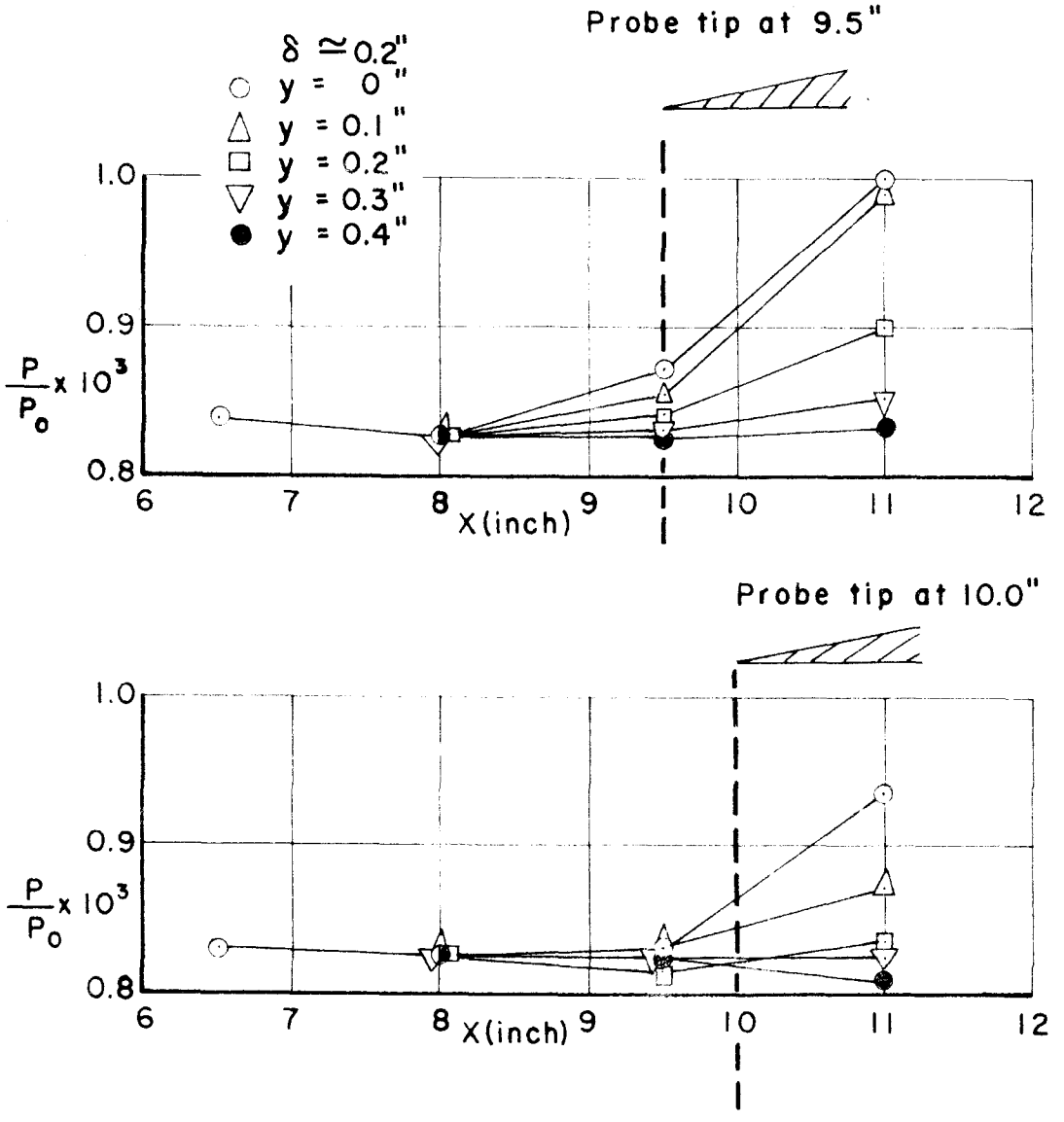

FIG. 15 – VARIATION OF PLATE SURFACE PRESSURE P/P_0 DISTRIBUTION WITH DISTANCE y OF HOT-WIRE PROBE ABOVE SURFACE.

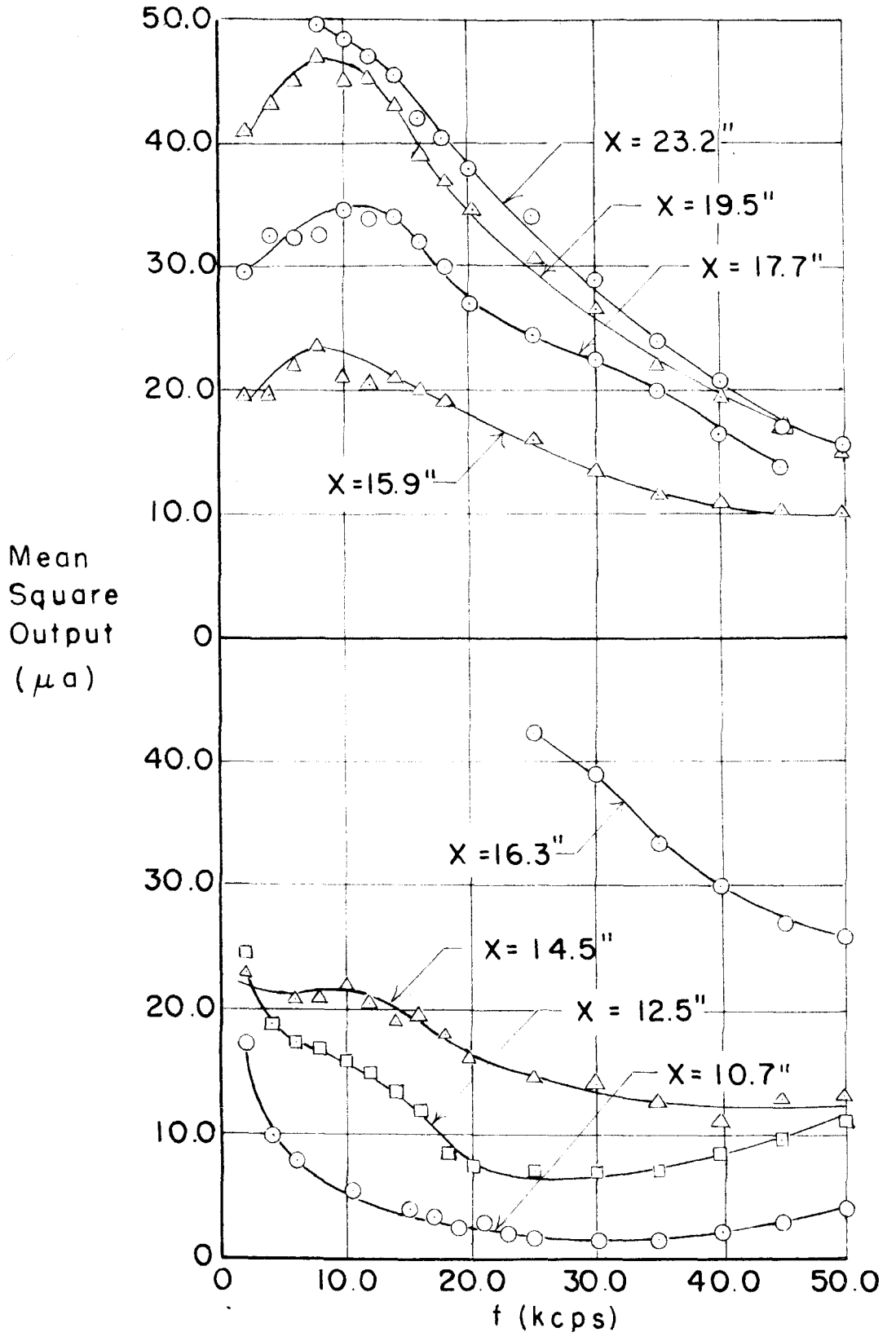

FIG. 16-VARIATION OF FLUCTUATION ENERGY SPECTRUM WITH POSITION ALONG TUNNEL CENTERLINE. P_0 = 50 psig

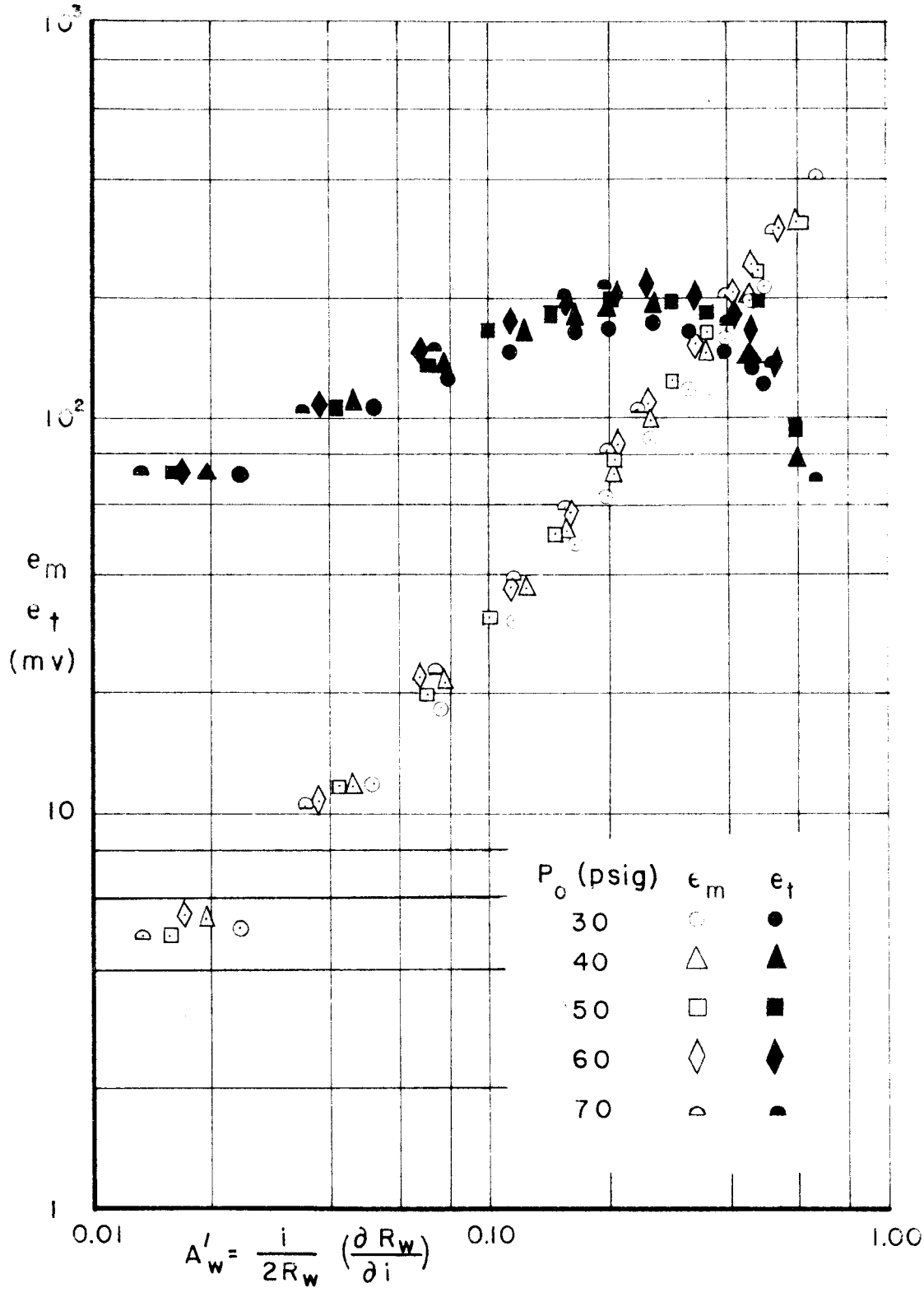

FIG. 17 – VARIATION OF HOT-WIRE SENSITIVITY COEFFICIENTS IN HYPERSONIC FLOW. $M = 5.8$, $T_0 = 225°F$

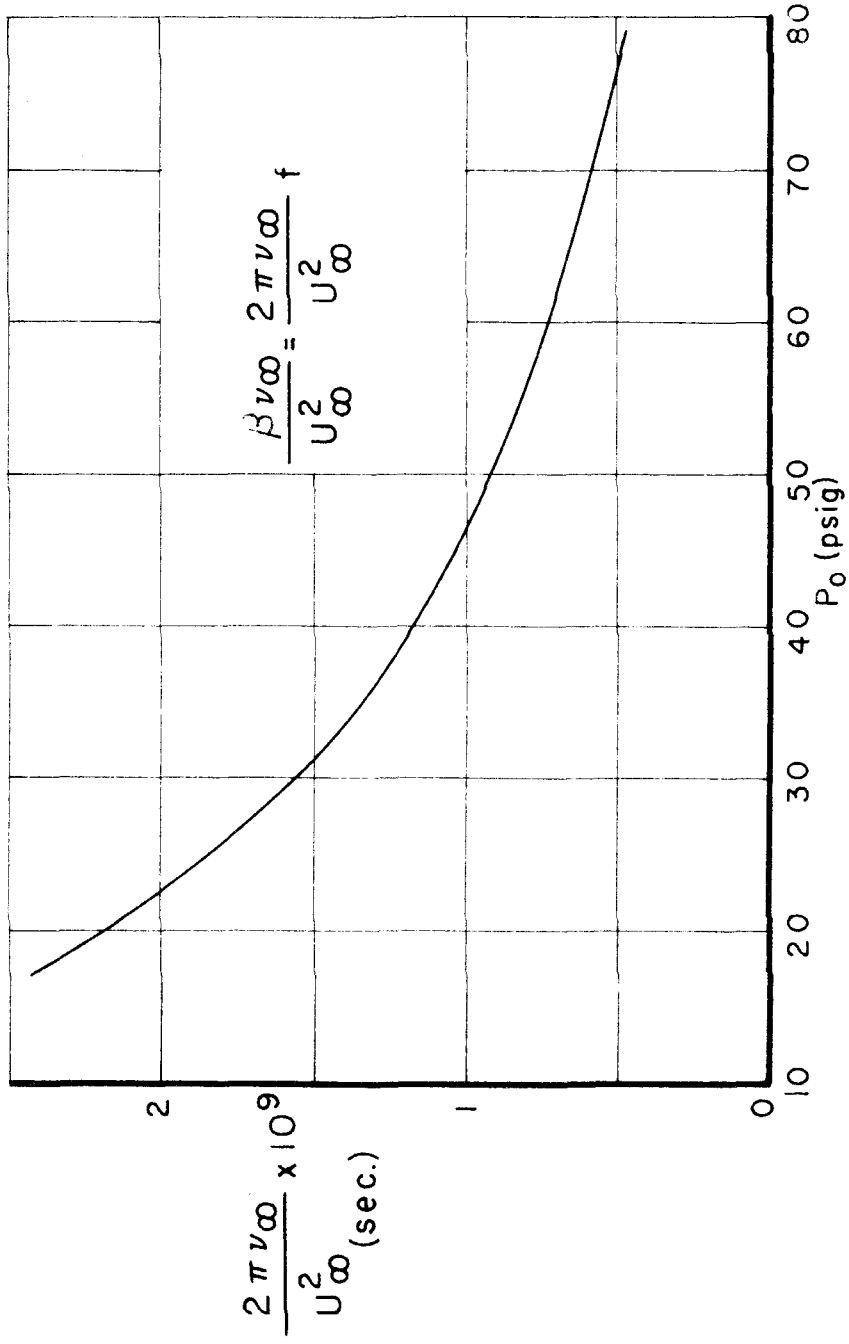

FIG. 18 – VARIATION OF THE PARAMETER $2\pi\nu_\infty/U_\infty^2$ WITH SUPPLY PRESSURE FOR M = 5.8 AND T_0 = 225° F

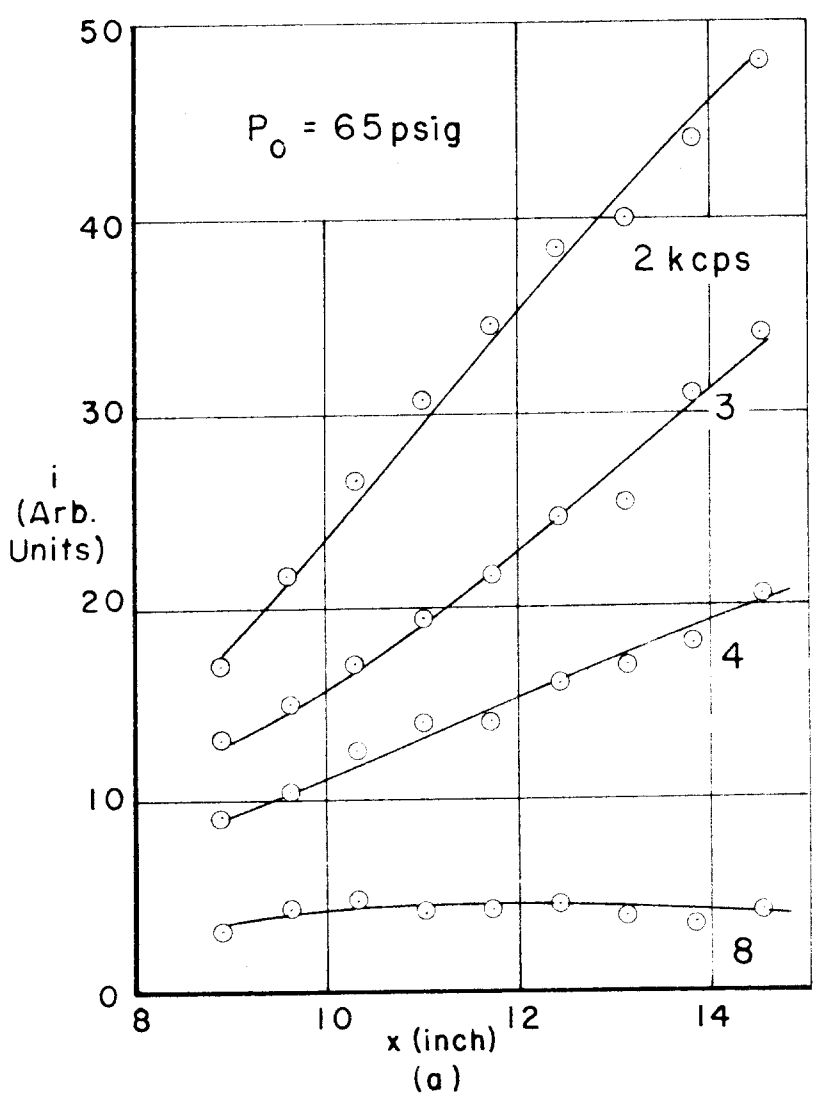

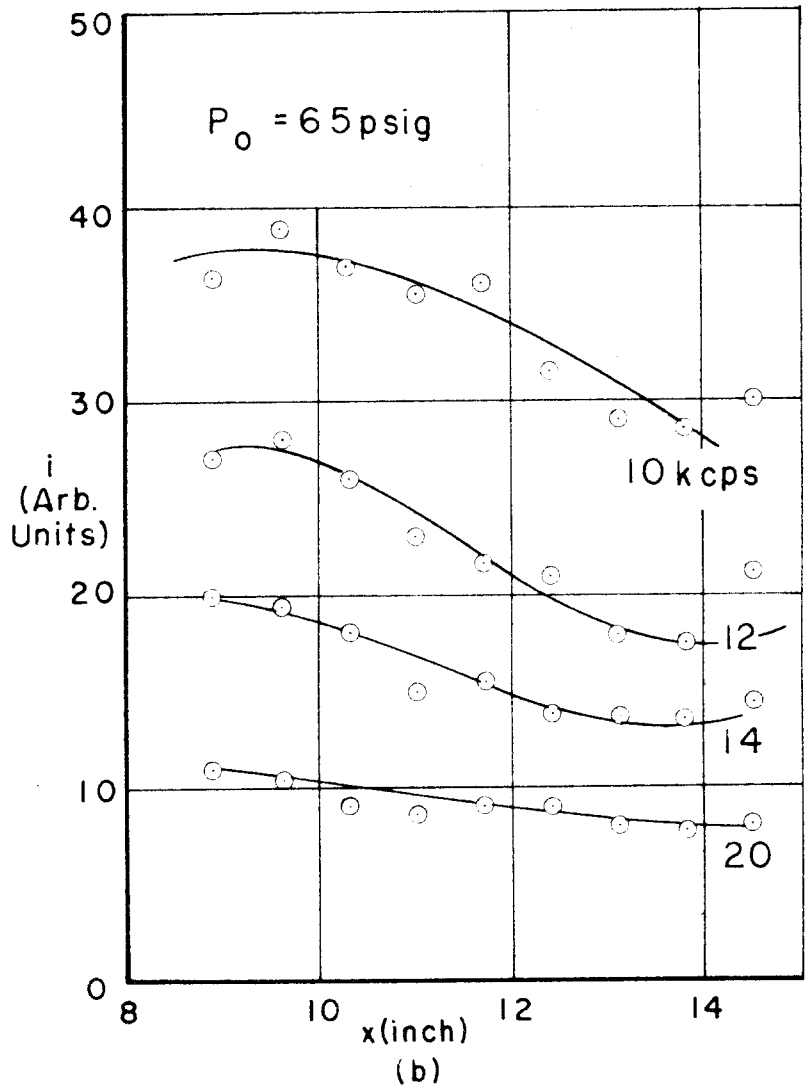

FIG. 19 – TYPICAL HOT-WIRE OUTPUT INTENSITY VARIATIONS DUE TO NATURAL FLUCTUATIONS

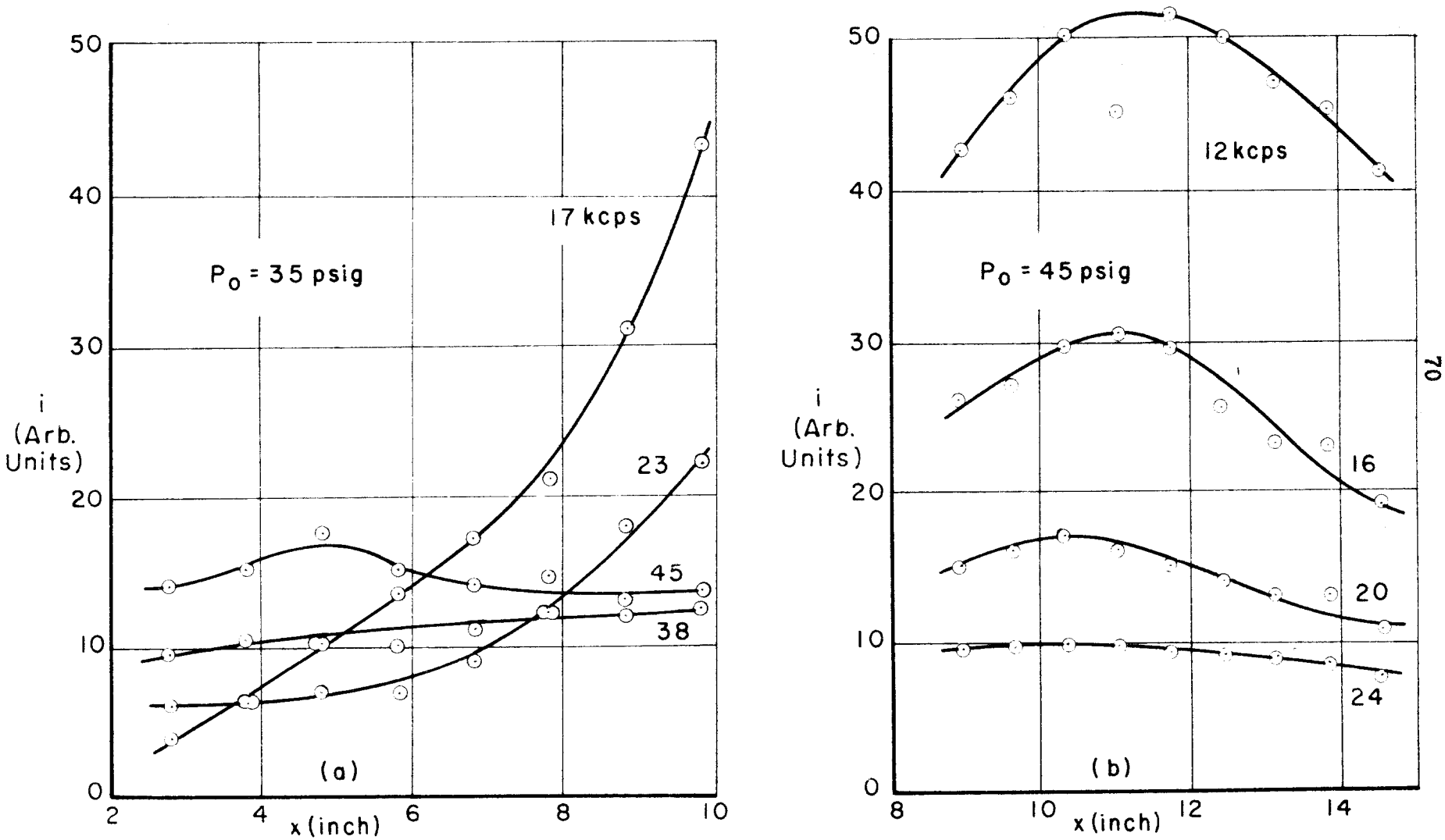

FIG. 20-TYPICAL VARIATION OF HOT-WIRE OUTPUT INTENSITY DUE TO NATURAL FLUCTUATIONS

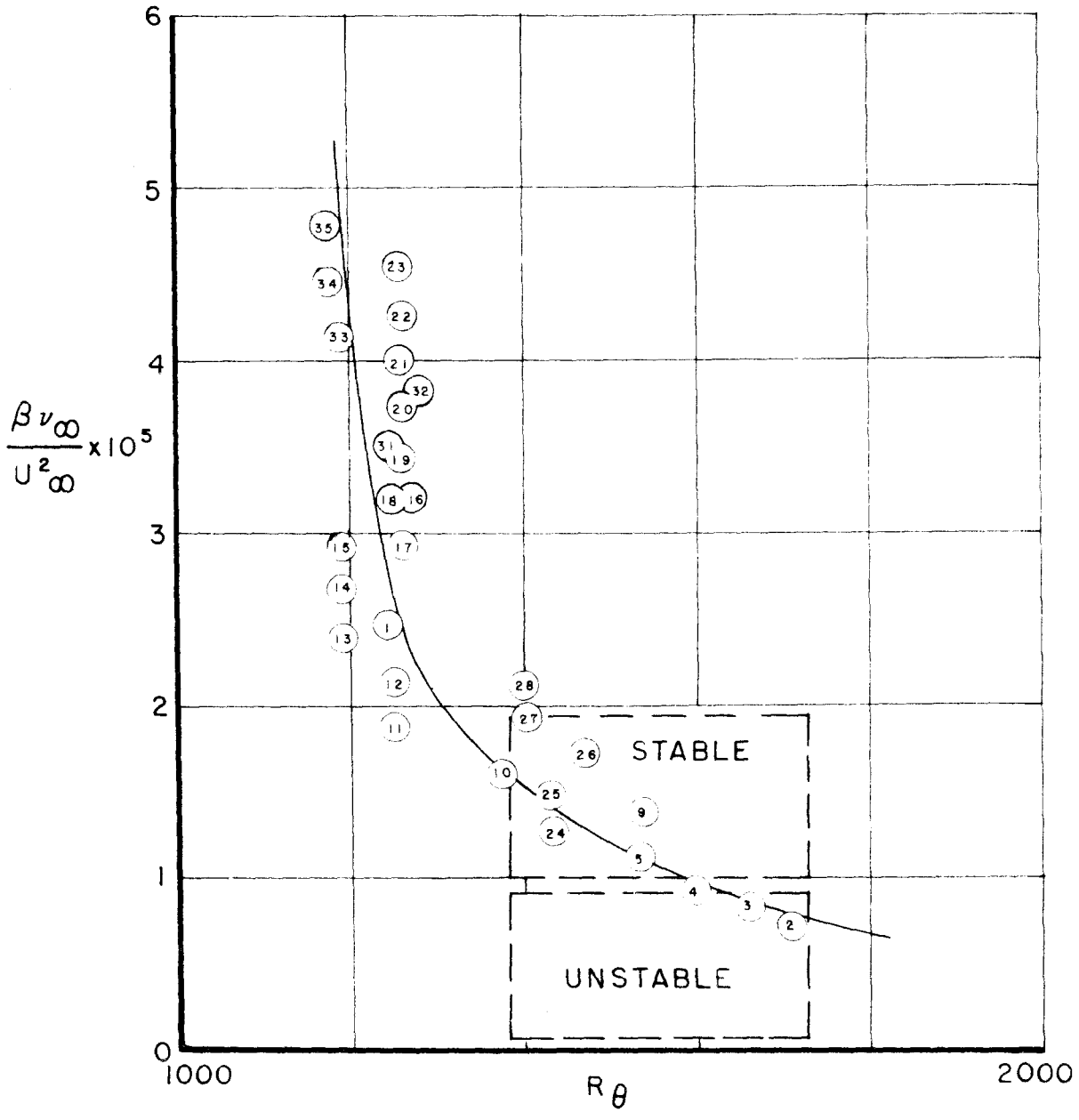

FIG. 21 - THE LOCUS OF MAXIMA (UPPER NEUTRAL BRANCH) IN THE AMPLITUDE VARIATION OF NATURAL FLUCTUATIONS. NUMBERS IDENTIFY DATA POINTS OF TABLE 2

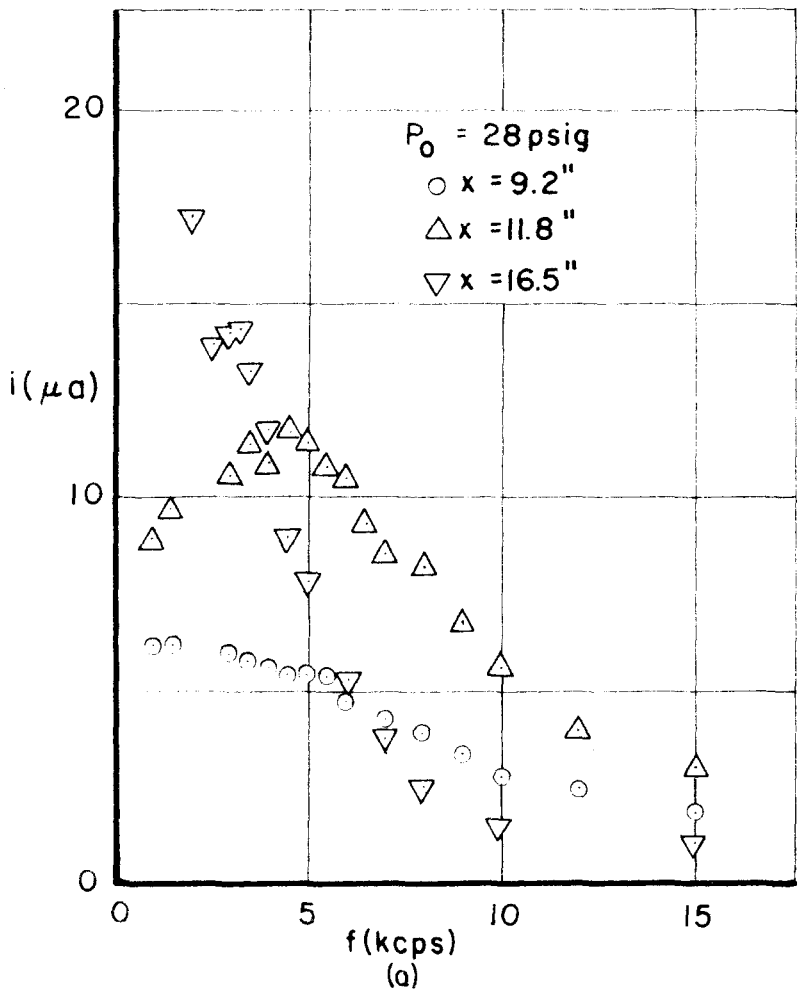

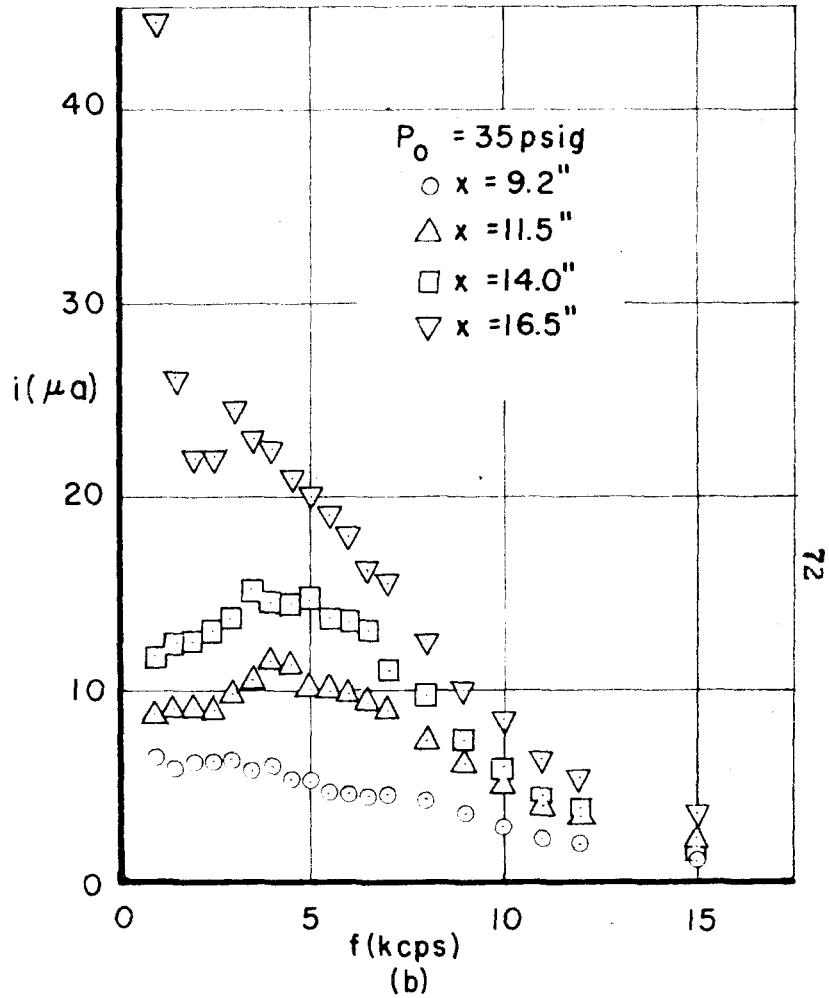

FIG. 22 – HOT-WIRE MEAN-SQUARE OUTPUT SPECTRA IN THE LAMINAR BOUNDARY LAYER

$M = 5.8$, $T_o = 225°$ F

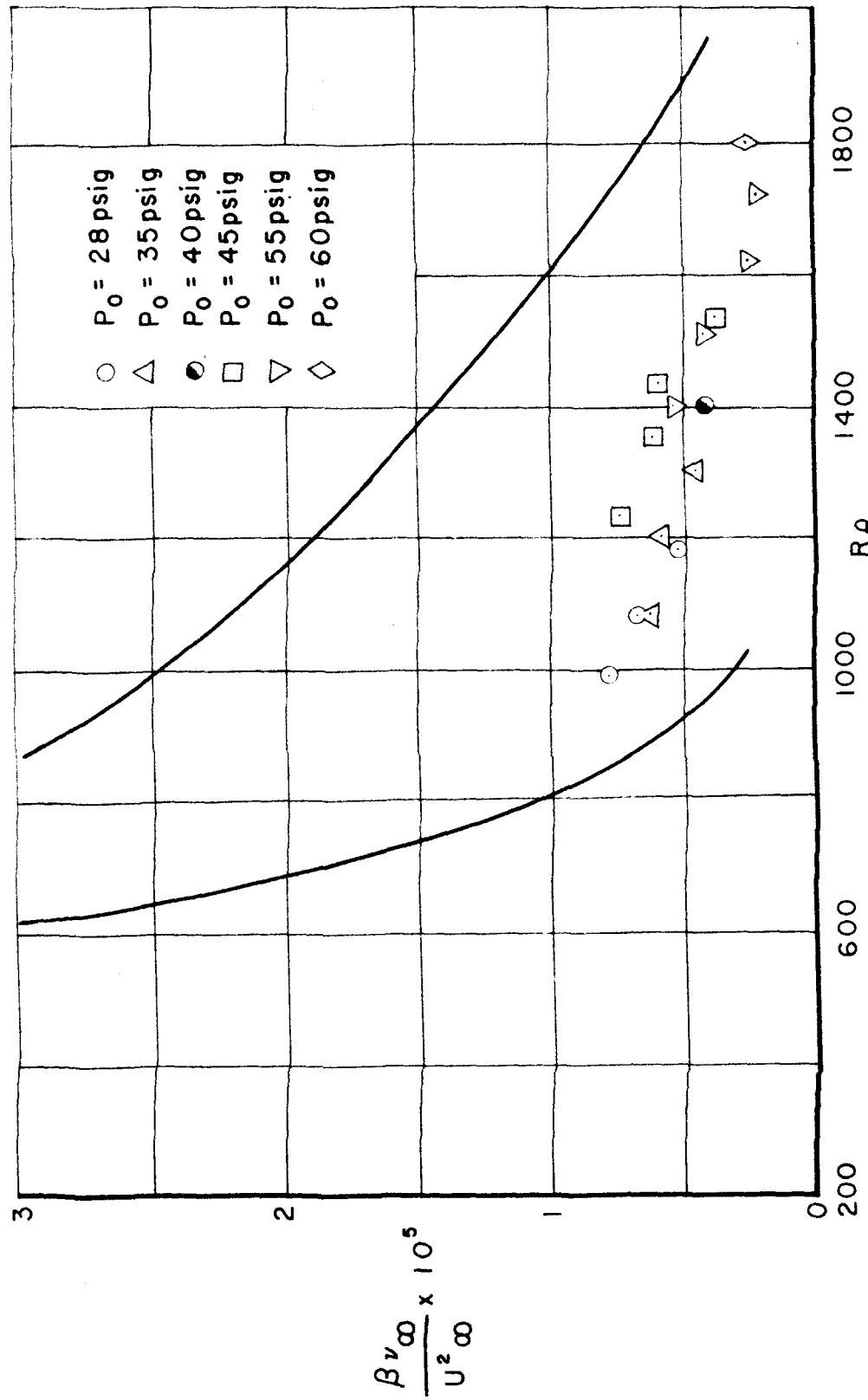

FIG. 23 - POINTS DEFINING THE "LINE OF MAXIMUM AMPLIFICATION

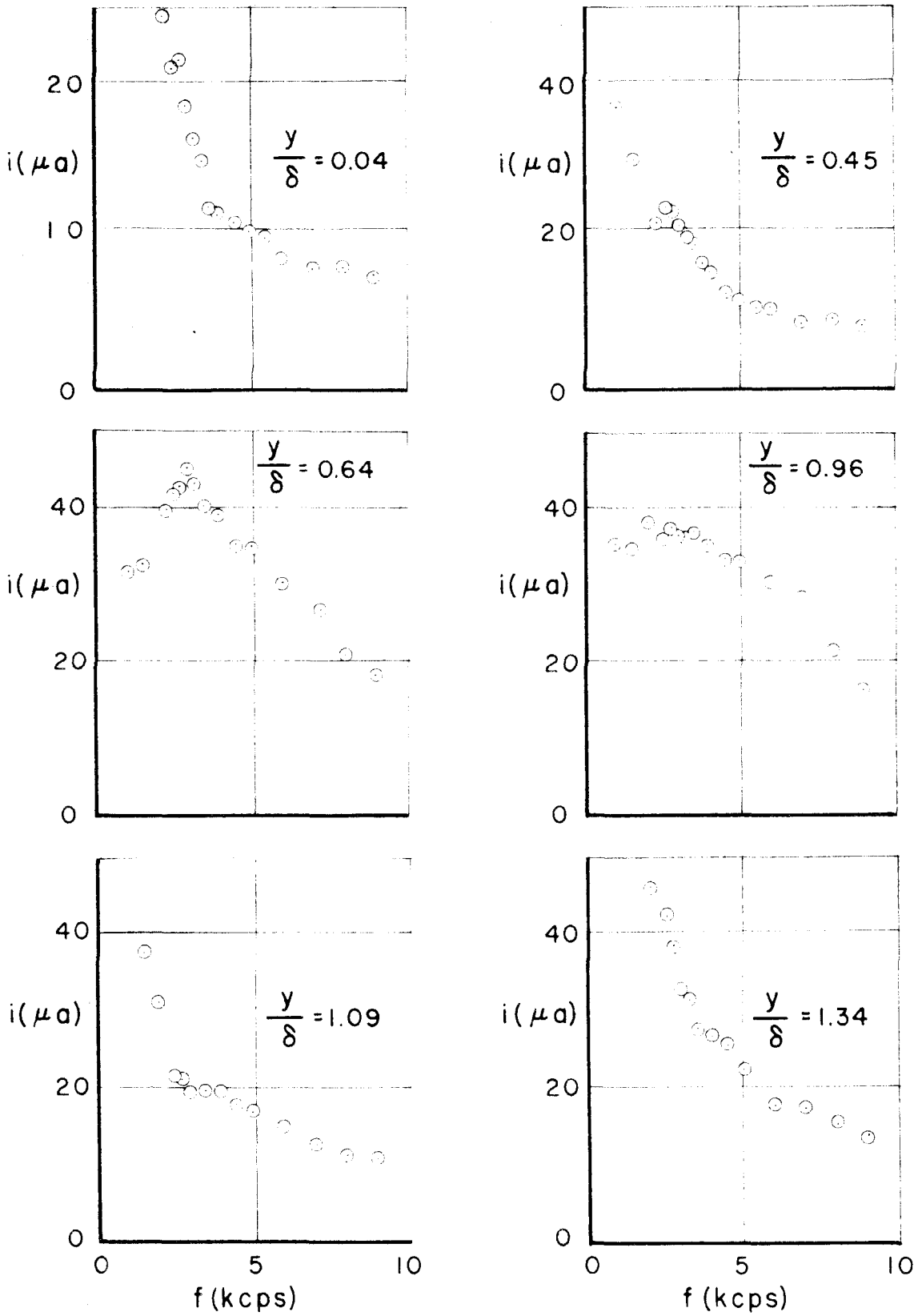

FIG. 24 – TYPICAL VARIATION OF HOT-WIRE MEAN-SQUARE OUTPUT SPECTRUM ACROSS LAYER AT $R_\theta \simeq 1400$

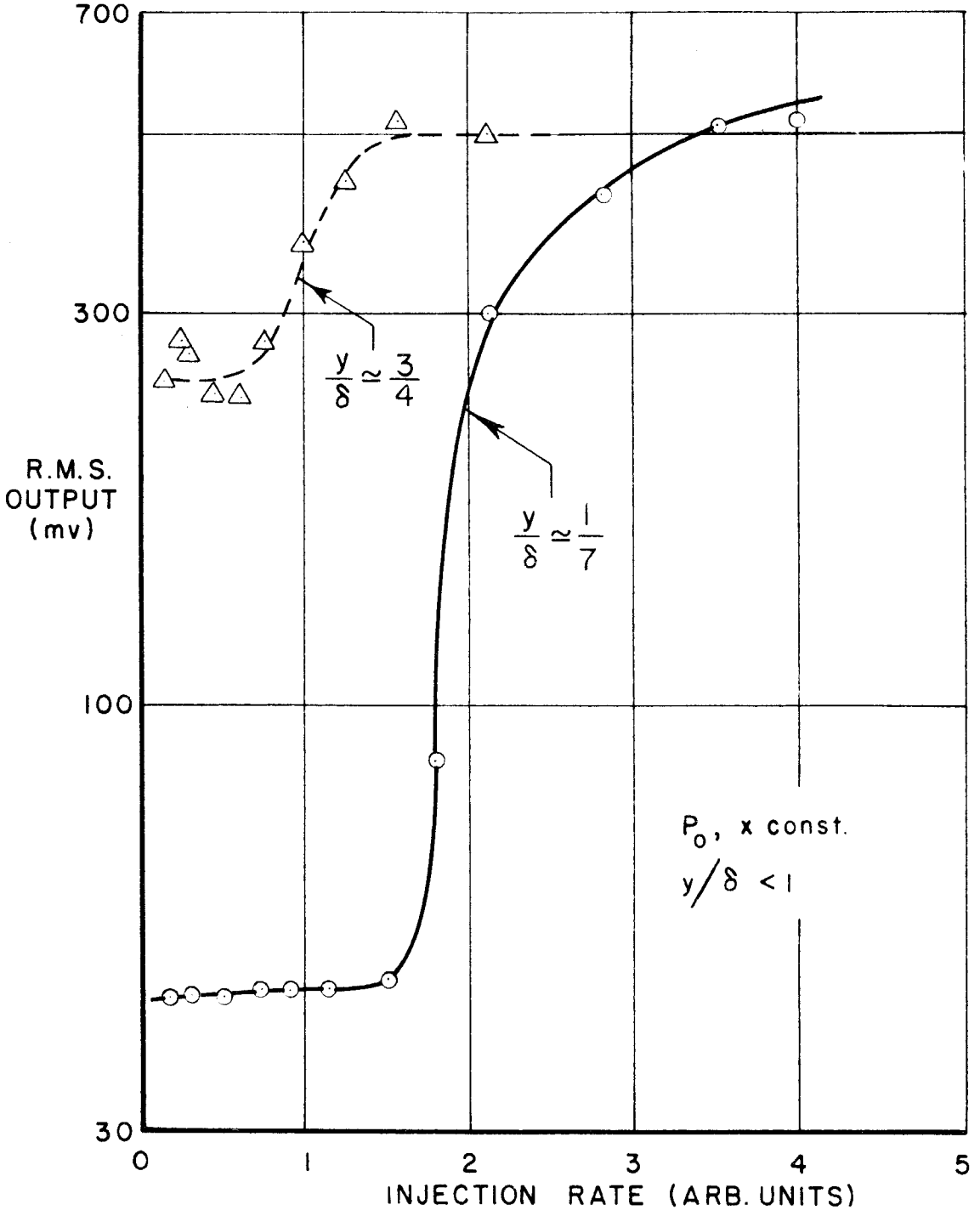

FIG. 25—TYPICAL RESPONSE OF THE HOT-WIRE AT LOCATION (x, y) TO AIR INJECTION THROUGH THE SIREN SLIT

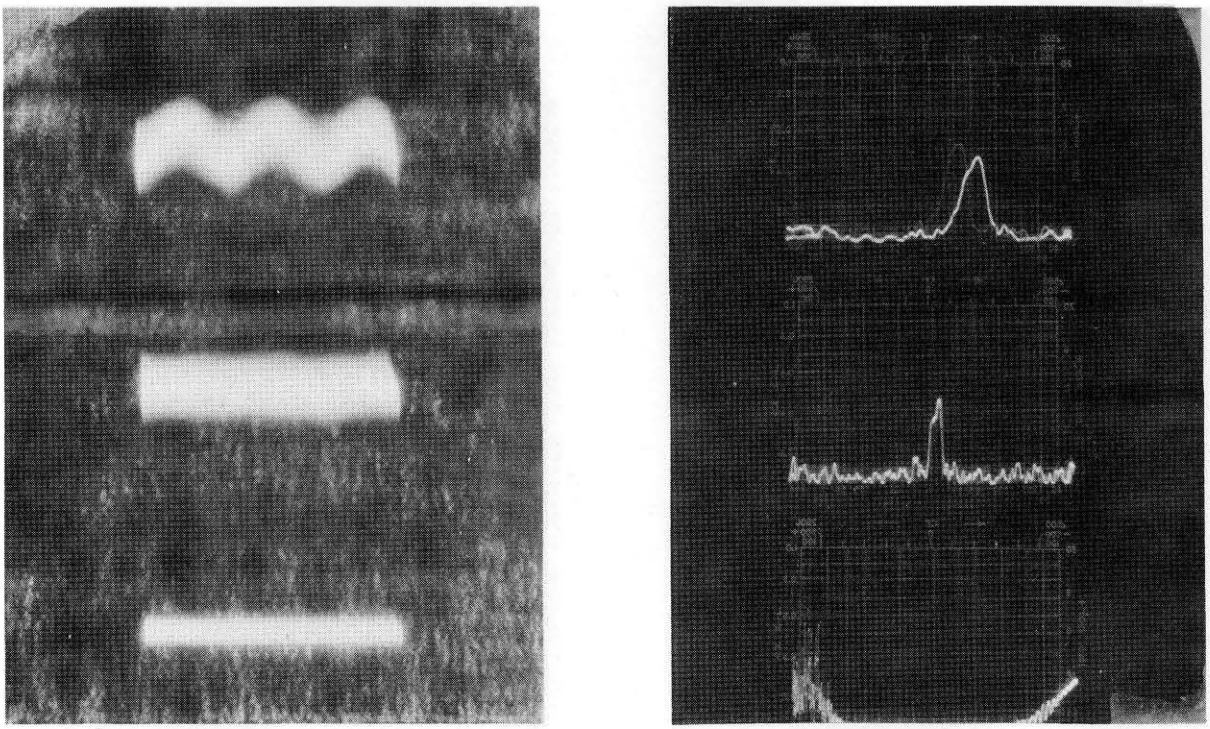

FIGURE 26

ASPECT OF THE FLUCTUATIONS INDUCED INTO THE LAMINAR HYPERSONIC BOUNDARY LAYER WITH THE SIREN MECHANISM

At left are shown oscilloscope traces of the hot-wire output with the siren injecting a 15 kcps fluctuation (upper trace), the effect of stopping the siren (middle trace) and the electronic noise in the system (bottom trace). At right is shown the same fluctuation as viewed with the display-type wave-analyzer (top two traces). The ordinate represents signal intensity and the abcissa, contracted in the middle trace, the frequency.

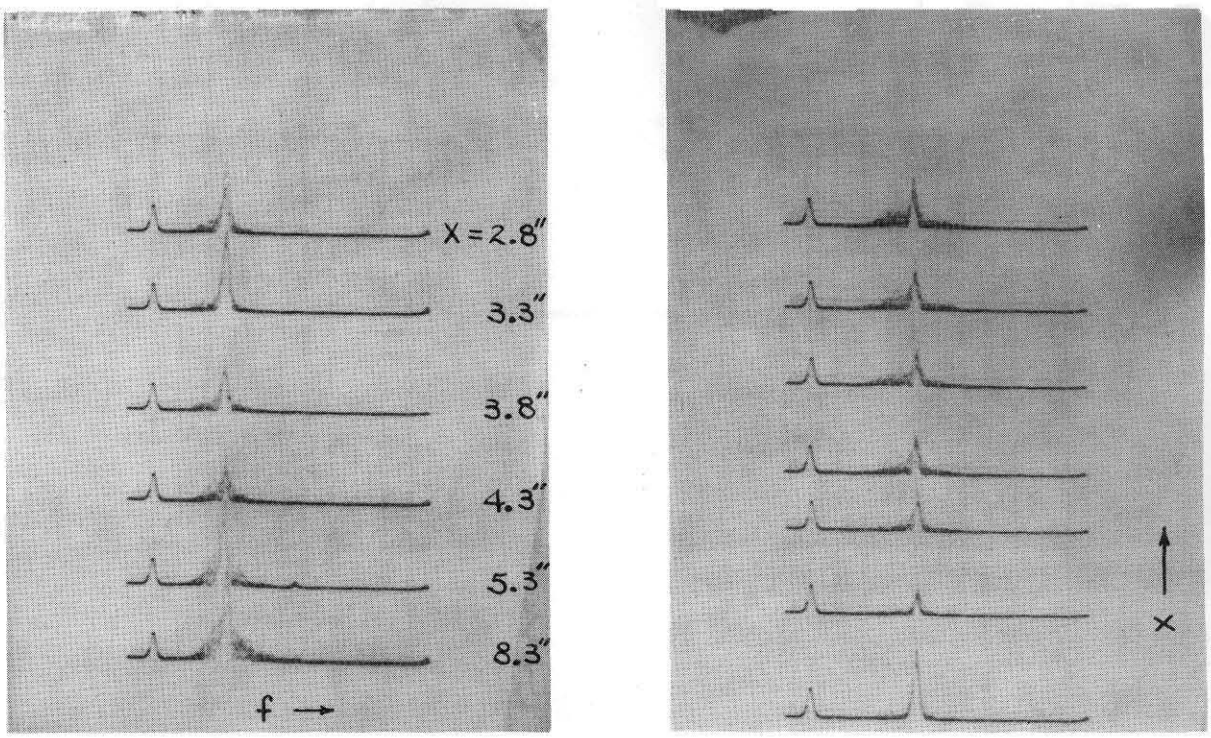

FIGURE 27

VARIATION IN THE AMPLITUDE OF THE ARTIFICIAL FLUCTUATIONS WITH POSITION OF x OF THE WIRE IN THE BOUNDARY-LAYER AS VIEWED WITH THE DISPLAY-TYPE WAVE ANALYZER

P_o = 40 psig; y/δ = 0.9; f = 5.5 kcps (left) and 8 kcps (right)

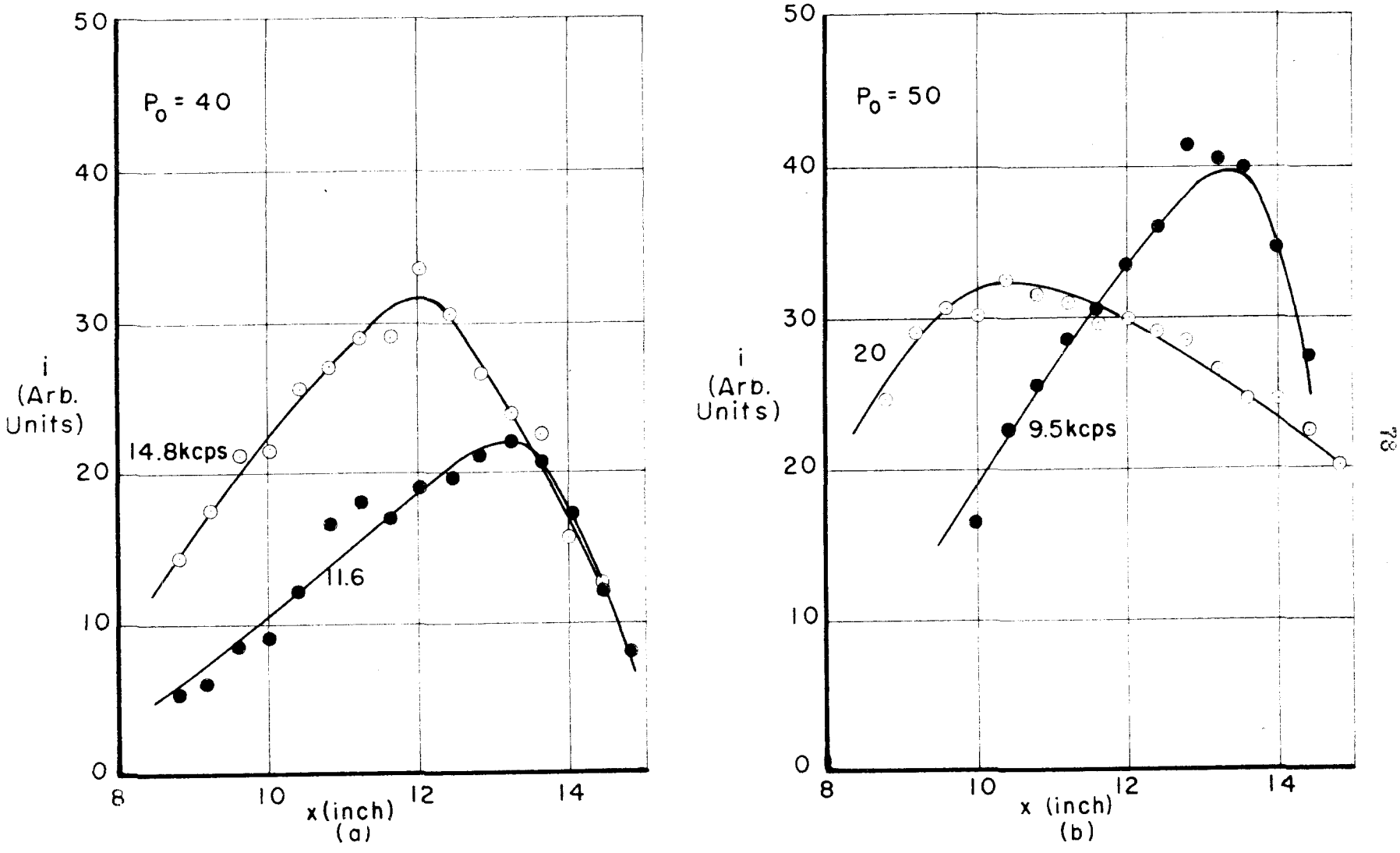

FIG. 28 – TYPICAL HOT-WIRE OUTPUT VARIATIONS DUE TO ARTIFICIAL FLUCTUATIONS

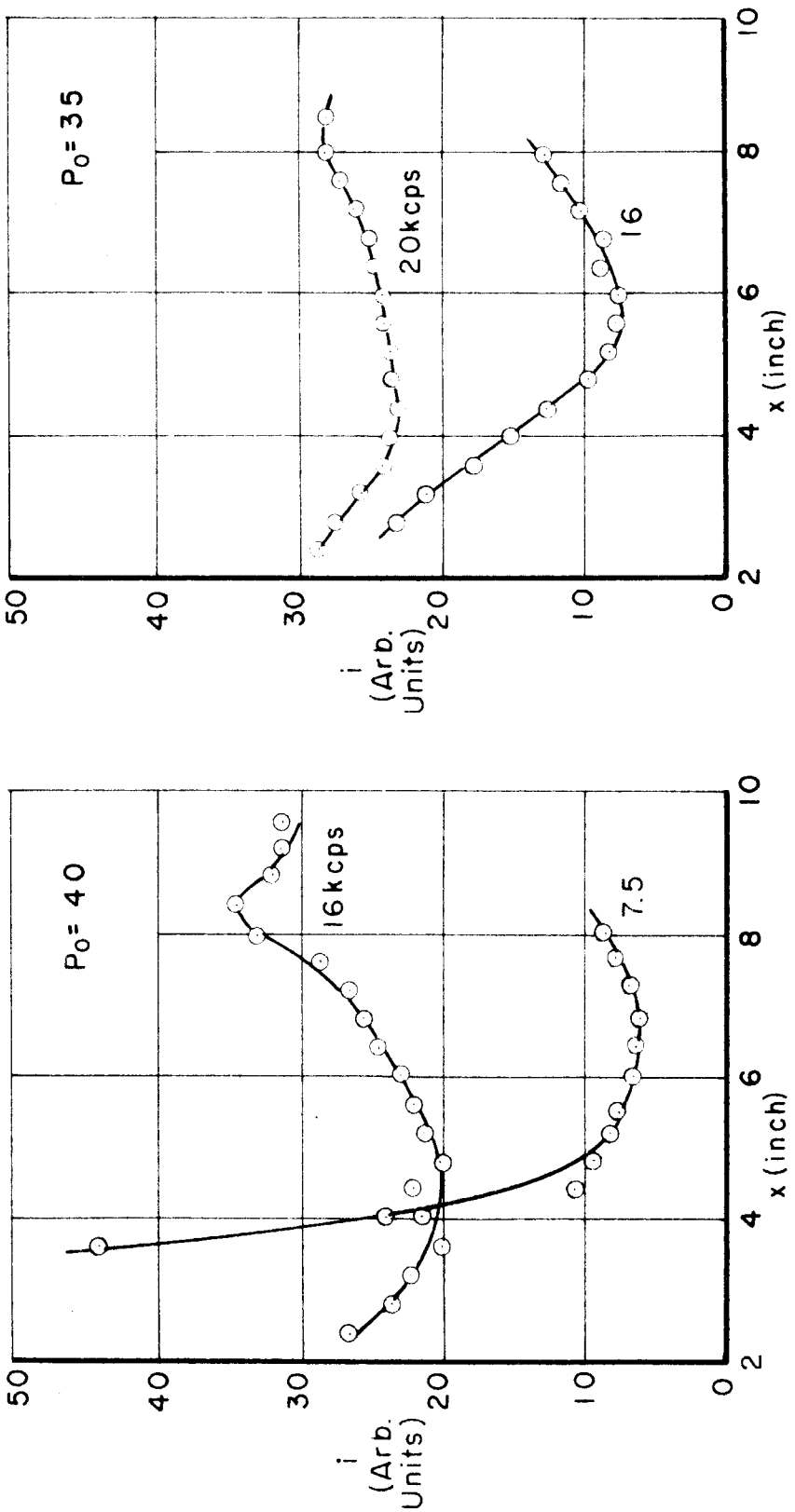

FIG. 29 – TYPICAL HOT-WIRE OUTPUT VARIATIONS DUE TO ARTIFICIAL FLUCTUATIONS

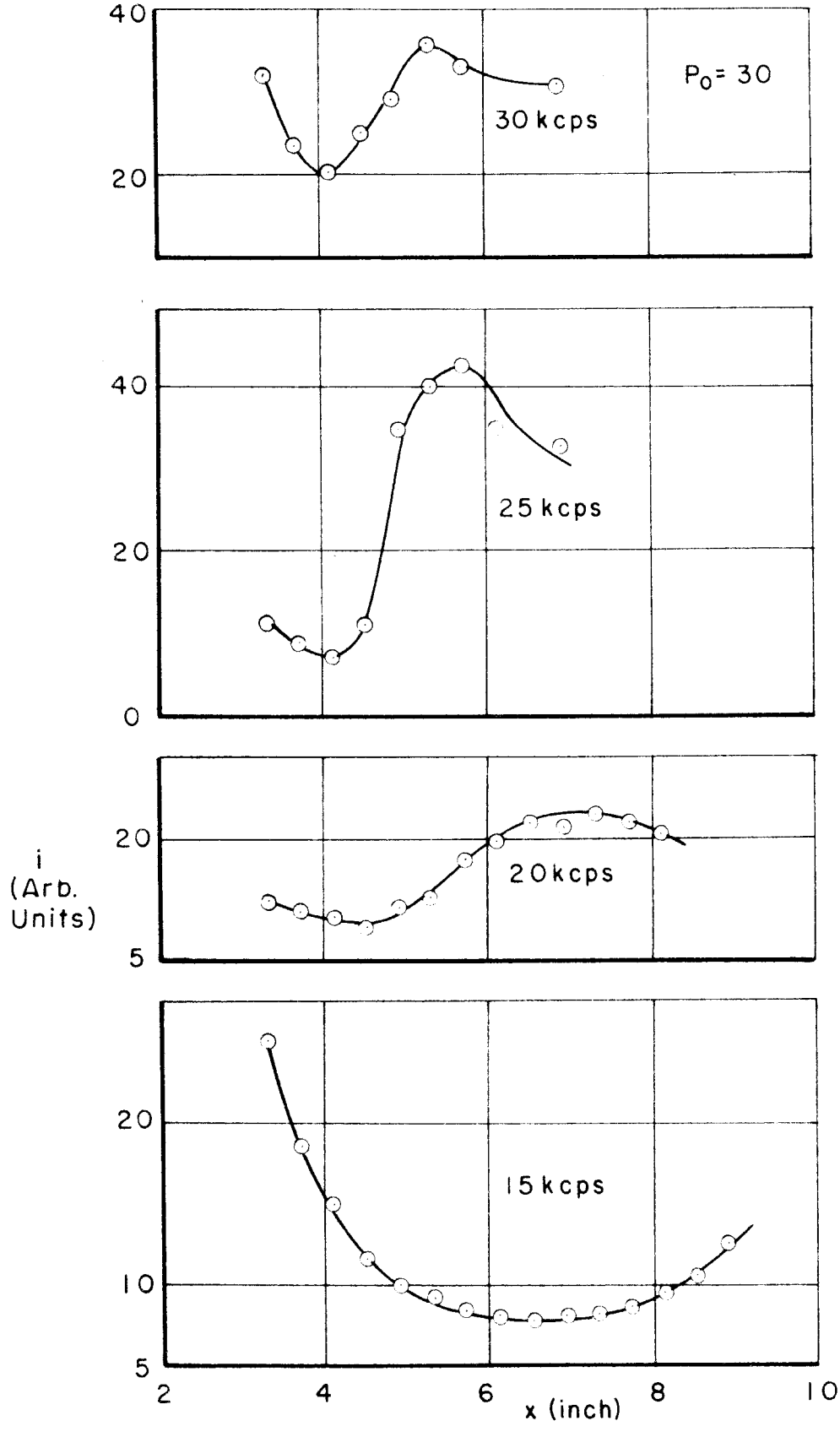

FIG. 30 - TYPICAL HOT-WIRE OUTPUT VARIATIONS DUE TO ARTIFICIAL FLUCTUATIONS

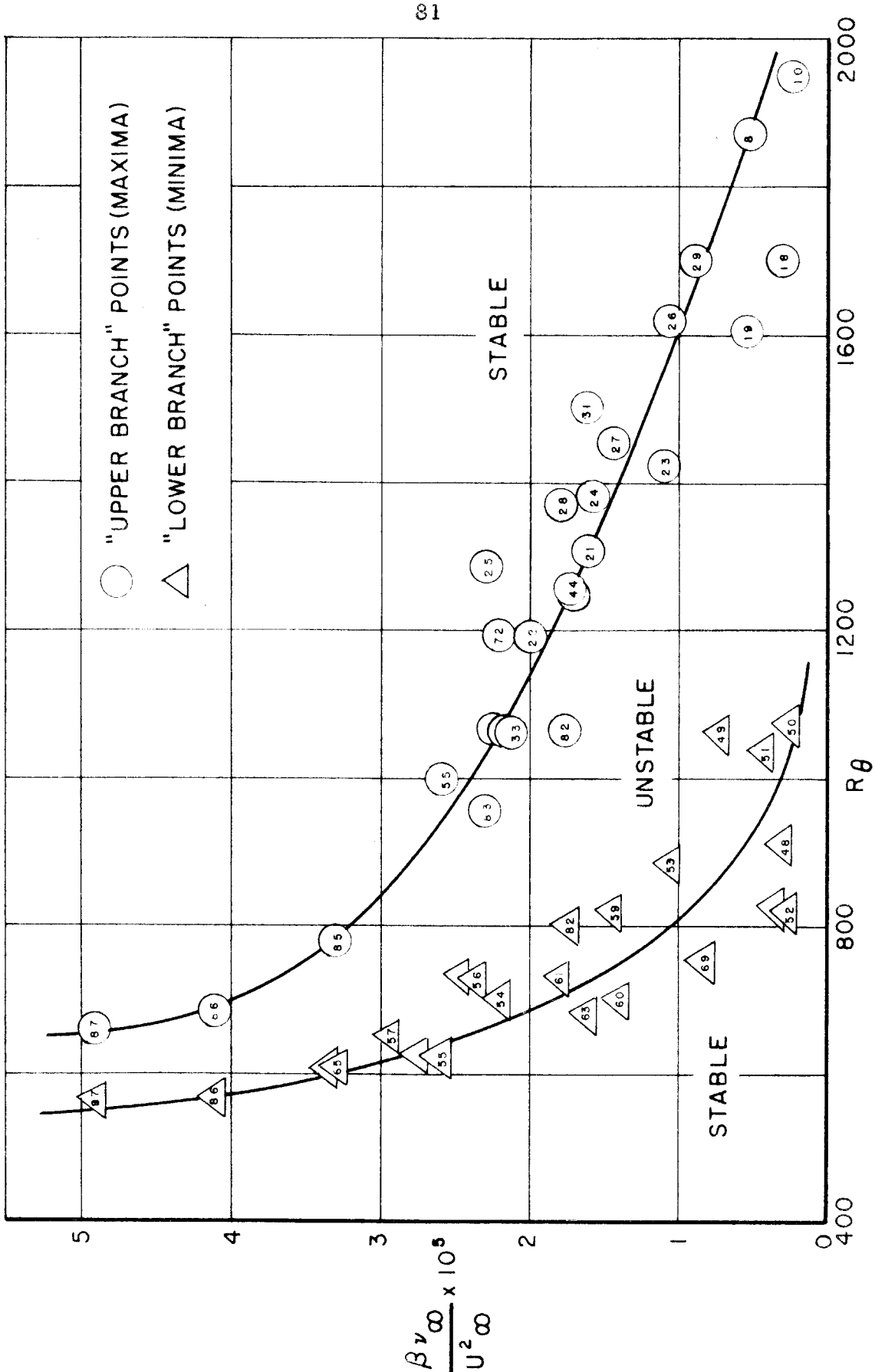

FIG. 31 – UPPER AND LOWER NEUTRAL STABILITY BRANCHES FOR ARTIFICIAL FLUCTUATIONS

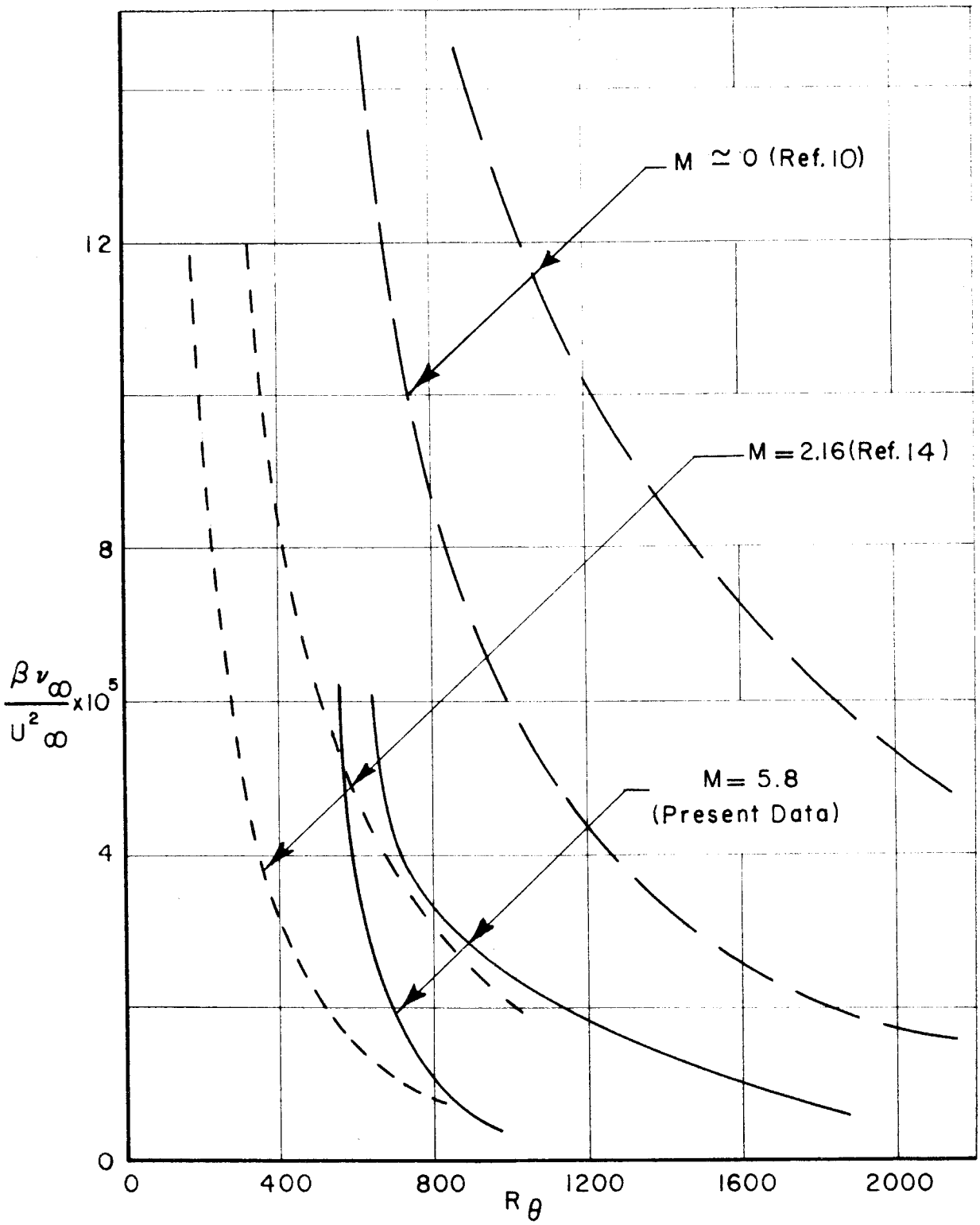

FIG. 32 - EXPERIMENTALLY DETERMINED BOUNDARY-LAYER STABILITY FOR VARIOUS MACH NUMBERS

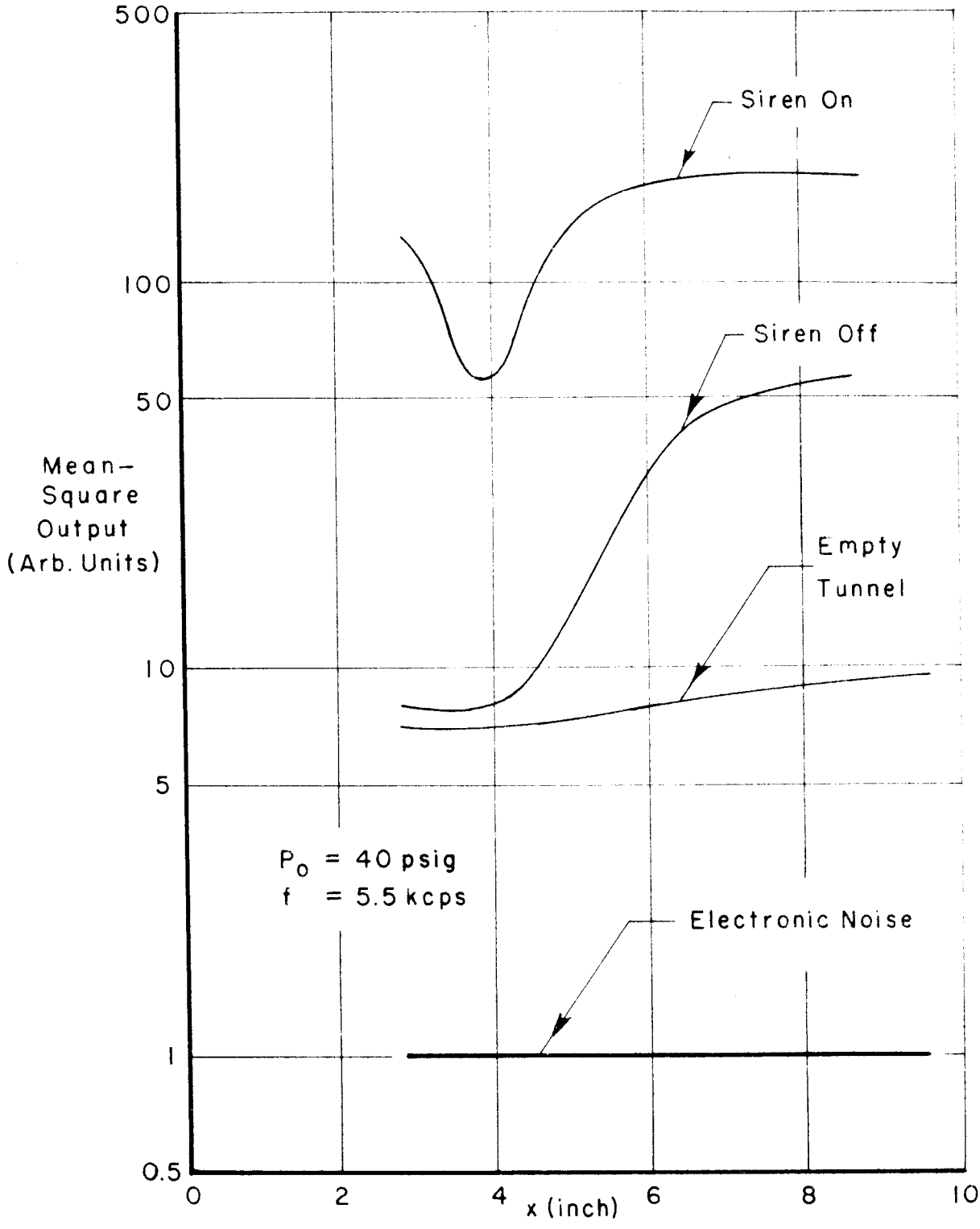

FIG. 33 — COMPARISON OF SIGNAL LEVEL AND DISTRIBUTION WITH AND WITHOUT THE SIREN AND WITHOUT THE FLAT PLATE

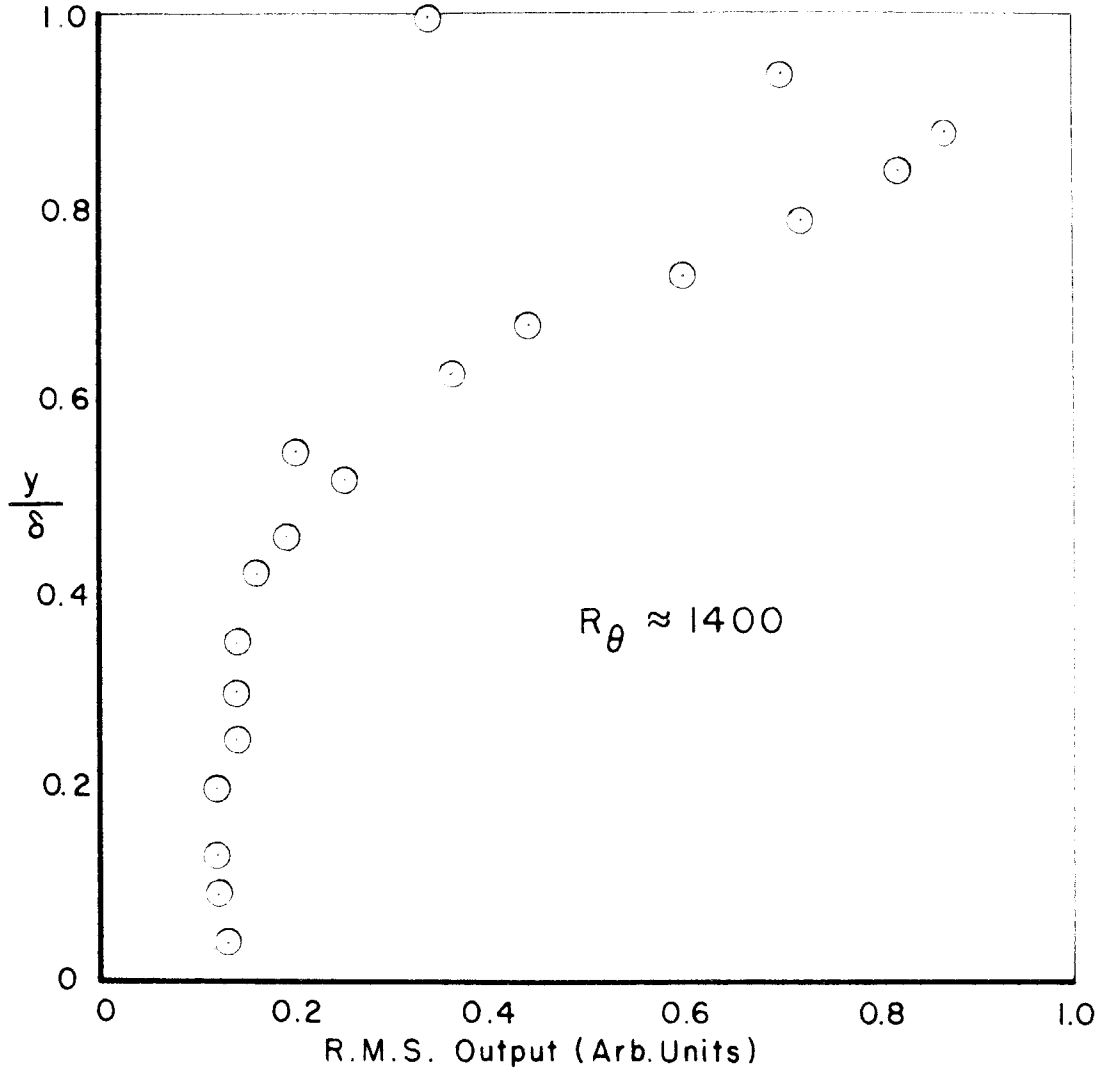

FIG. 34 - VARIATION ACROSS THE LAMINAR BOUNDARY LAYER OF THE HOT-WIRE OUTPUT INTEGRATED OVER ALL FREQUENCIES

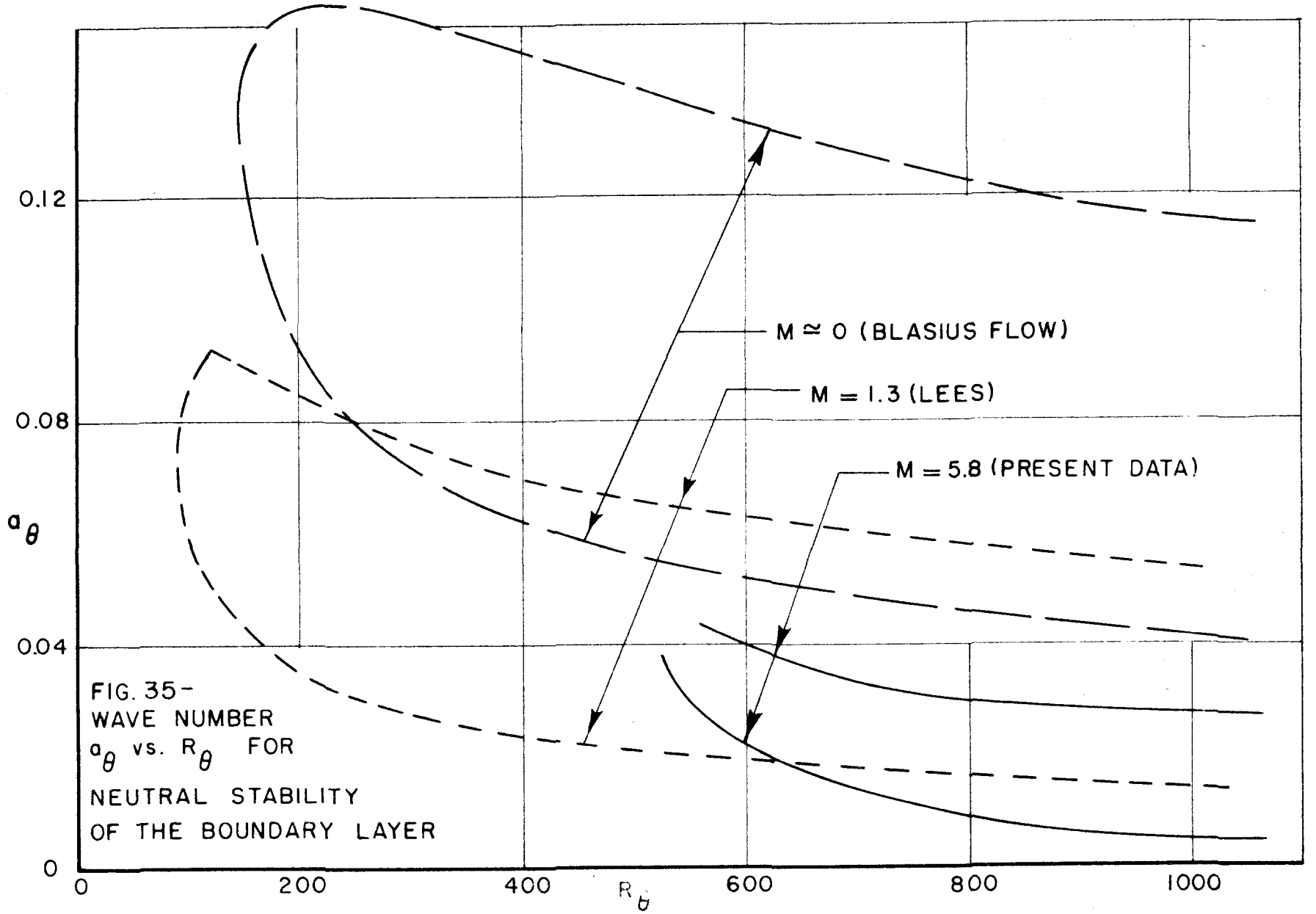

FIG. 35–
WAVE NUMBER
a_θ vs. R_θ FOR
NEUTRAL STABILITY
OF THE BOUNDARY LAYER